

Demographic History and Genomic Response to Environmental Changes in a Rapid Radiation of Wild Rats

Deyan Ge ^{†,1} Anderson Feijó,^{†,1} Zhixin Wen,¹ Alexei V. Abramov,^{2,3} Liang Lu,⁴ Jilong Cheng,¹ Shengkai Pan,⁵ Sicheng Ye,⁶ Lin Xia,¹ Xuelong Jiang,⁷ Alfried P. Vogler,^{*} ^{8,9} and Qisen Yang^{*,1}

¹Key Laboratory of Zoological Systematics and Evolution, Institute of Zoology, Chinese Academy of Sciences, Chaoyang District, Beijing, China

²Zoological Institute, Russian Academy of Sciences, Saint Petersburg, Russia

³Joint Russian-Vietnamese Tropical Research and Technological Centre, Hanoi, Vietnam

⁴State Key Laboratory for Infectious Diseases Prevention and Control, National Institute for Communicable Disease Control and Prevention, Chinese Center for Disease Control and Prevention, Beijing, China

⁵CAS Key Lab of Animal Ecology and Conservation Biology, Institute of Zoology, Chinese Academy of Sciences, Beijing, China

⁶Center for Computational Genomics, Beijing Institute of Genomics, Chinese Academy of Sciences, Beijing, China

⁷State Key Laboratory of Genetic Resources and Evolution, Kunming Institute of Zoology, Chinese Academy of Sciences, Kunming, Yunnan, China

⁸Department of Life Sciences, Natural History Museum, London, United Kingdom

⁹Department of Life Sciences, Imperial College London, Silwood Park Campus, Ascot, United Kingdom

[†]These authors contributed equally to this work.

***Corresponding authors:** E-mails: a.vogler@imperial.ac.uk; yangqs@ioz.ac.cn.

Associate editor: Bing Su

Abstract

For organisms to survive and prosper in a harsh environment, particularly under rapid climate change, poses tremendous challenges. Recent studies have highlighted the continued loss of megafauna in terrestrial ecosystems and the subsequent surge of small mammals, such as rodents, bats, lagomorphs, and insectivores. However, the ecological partitioning of these animals will likely lead to large variation in their responses to environmental change. In the present study, we investigated the evolutionary history and genetic adaptations of white-bellied rats (*Niviventer* Marshall, 1976), which are widespread in the natural terrestrial ecosystems in Asia but also known as important zoonotic pathogen vectors and transmitters. The southeastern Qinghai-Tibet Plateau was inferred as the origin center of this genus, with parallel diversification in temperate and tropical niches. Demographic history analyses from mitochondrial and nuclear sequences of *Niviventer* demonstrated population size increases and range expansion for species in Southeast Asia, and habitat generalists elsewhere. Unexpectedly, population increases were seen in *N. eha*, which inhabits the highest elevation among *Niviventer* species. Genome scans of nuclear exons revealed that among the congeneric species, *N. eha* has the largest number of positively selected genes. Protein functions of these genes are mainly related to olfaction, taste, and tumor suppression. Extensive genetic modification presents a major strategy in response to global changes in these alpine species.

Key words: phylogenomics, evolution, Murinae, micromammals, demographic history.

Introduction

Moving away, persisting via local adaptation or phenotypic plasticity, or extinction are the three outcomes of a natural population response to environmental changes (Chevin et al. 2010). To survive under environmental extremes requires to adapt through behavioral, morphological, or physiological means, and these may differ even among closely related species (Hoffmann and Sgro 2011). The effectiveness of these responses influences evolutionary dynamics, population demography, and ultimately the survival in the wild. Discovering the demographics and population genetics that coincide with

responses to environmental change and their underlying genetic adaptations are now major tasks in biological research (Franks and Hoffmann 2012). Development of sequencing technologies and data analysis methods now allows evolutionary reconstruction of the climate responses at the genome level.

The extinction and population decrease of large mammals since the late Quaternary have received much attention in recent scientific studies (Stuart et al. 2004; McClenachan et al. 2016). Megafaunal extinctions reshaped the structure of

© The Author(s) 2021. Published by Oxford University Press on behalf of the Society for Molecular Biology and Evolution.

This is an Open Access article distributed under the terms of the Creative Commons Attribution Non-Commercial License (<http://creativecommons.org/licenses/by-nc/4.0/>), which permits non-commercial re-use, distribution, and reproduction in any medium, provided the original work is properly cited. For commercial re-use, please contact journals.permissions@oup.com

Open Access

terrestrial ecosystems (Malhi et al. 2016; Galetti et al. 2018). Rodents, bats, lagomorphs, and insectivores are now the common and dominant mammal groups in most regions, and relative species richness of rodents is predicted to increase further within the next 50 years (Davis et al. 2018). Small mammals, particularly rodents, are also reservoirs and hosts for diverse zoonotic diseases (Guzzetta et al. 2017; Rabiee et al. 2018), and thus the population dynamics and range shifts of these species affect the origin and transmission of potential pathogens into humans. However, the evolutionary mechanisms that drive speciation and adaptation of these species remain poorly explored.

The recent population size dynamics and range expansion of commensal rodents, such as brown rats (*Rattus norvegicus*) (Deinum et al. 2015; Puckett et al. 2016; Teng et al. 2017; McClelland et al. 2018; Zeng et al. 2018; Suzuki et al. 2019) and house mice (*Mus musculus*) (Jing et al. 2014; McClelland et al. 2018), have largely been linked to activities and migrations of humans. These rodents are now the most successful invaders in the world, affecting human history by transferring plague, hantavirus, Anjzorobe virus, and others (Liu et al. 2017; Rabiee et al. 2018; Raharinosy et al. 2018). However, wild species closely related to these commensal rodents are abundant in nature and also play important roles as pathogen reservoirs and transmitters, whereas the population dynamics and range changes have been poorly explored. The lack of comprehensive field surveys and studies on the evolution and demographic history of these species may leave humans unprepared to epidemic outbreaks.

White-bellied rats (*Niviventer* Marshall, 1976) are among the most speciose and dominant mammals in forest ecosystems from Southeast Asia to North China. Previous studies clarified the phylogenetic relationships and taxonomy of different species complexes in this genus, with approximately 23 species recognized (Musser 1981; Musser and Carleton 2005; Denys et al. 2016; Zhang, He, et al. 2016; Ge et al. 2018; Ge, Feijó, et al. 2020). These species have shown rapid speciation since the late Miocene (Lu et al. 2015; Zhang, He, et al. 2016) and are ideal taxa for studying the adaptive evolution of terrestrial mammals that diversified in one of the most complex geological environments on Earth. Species of *Niviventer* serve as vectors of hantavirus (Wang et al. 2000; Cao et al. 2010; Lin et al. 2012; Hu et al. 2014; Ge et al. 2016; Dai et al. 2019), Lyme disease-related *Borrelia* (Masuzawa et al. 2001), Tsutsugamushi disease caused by *Rickettsia tsutsugamushi* (Latif et al. 2017), and *Babesiosis*, a tick-borne disease (Saito-Ito et al. 2008), among others. Ambiguity in the demographic history of these animals impedes a comprehensive understanding of their current status and may bias future monitoring of their population dynamics.

In the present study, we aimed to infer the demographic histories of *Niviventer* species combining coalescence methods and environmental range reconstructions under late Quaternary climate change. These individual scenarios are placed in a phylogenetic framework that establishes transitions in habitat association, in particular with regard to the altitudinal range of each species. Whole-genome data for each species then illuminate the primary genetic differences

underlying the evolutionary dynamics of these range shifts. Combined with the information on demographic and phylogenetic history, these data can address fundamental questions about the genomic basis of range shifts, and in particular the effect of shifts to extreme conditions at high altitude, compared with generalist species with wider climatic amplitude. Establishing which genes are under positive selection in species associated with different climatic range, allows inferences about the genomic basis of habitat shifts in an important adaptive radiation, and can help answering the question of how wild rats will respond to climatic changes in future.

Results

Phylogeny, Origin, Hybridization, and Divergence Time of *Niviventer*

Mitochondrial cytochrome b (*CYTB*) gene from 1,304 individuals including 117 sequences newly generated in the presented study was used in phylogenetic analyses (supplementary table 1, Supplementary Material online). Moreover, we shotgun sequenced the genome of 15 *Niviventer* species, two species of *Chiromyscus*, and *R. andamanensis* at 14× coverage on an average (38.68 ± 4.18 Gb, range 32.11–45.94, corresponding to 11.7–16.7× genome size of *R. norvegicus*). Phylogenetic reconstructions were based either on the *CYTB* gene alone, 13 protein-coding genes of the mitochondrial genome (MTG), or the single-copy orthologs (SCOs) extracted from autosomal scaffolds (supplementary tables 1–3, Supplementary Material online). Between 1,812 and 3,448 SCOs were identified for each sequenced *Niviventer* species. For MTG and SCOs, we reconstructed the phylogeny of *Niviventer* by using concatenation of all genes. Moreover, for the SCOs, we estimated species trees using unrooted gene trees under the multispecies coalescent model to account for incomplete lineage sorting. All analyses supported the monophyly of *Niviventer* (fig. 1 and supplementary figs. 1A and 2A, Supplementary Material online), with *Chiromyscus* as its sister taxon based on *CYTB*, but two species of *Chiromyscus* presented as paraphyletic using MTG and SCOs with regard to *Niviventer*. Phylogeny reconstructed using SCOs by concatenation and ASTRAL (Zhang et al. 2018) are similar in phylogenetic structure, which recognized the sister relationship of NESG and NASC (fig. 1).

Within *Niviventer* (fig. 1), four species complexes identified previously were found to be monophyletic: 1) the *N. eha* species complex (NESG, *N. eha* and *N. brahma*), endemic to the mountainous regions of the southeastern Qinghai-Tibet Plateau (QHTP) and western Yunnan and inhabiting the highest elevation among all extant wild murids; 2) the *N. andersoni* species complex (NASG, *N. andersoni* and *N. excelior*), distributed at middle to high elevations on the southeastern and southwestern QHTP, and in the Qingling Mountains and southeastern Wuling Mountains; 3) the *N. niviventer* species complex (NNSG, *N. bukit*, *N. confucianus*, *N. tenaster*, *N. niviventer*, *N. pianmaensis*, *N. gladiusmaculus*, *N. culturatus*, *N. coninga*, *N. lotipes*, etc.), widely distributed in Southeast Asia, from the southeastern QHTP to North of

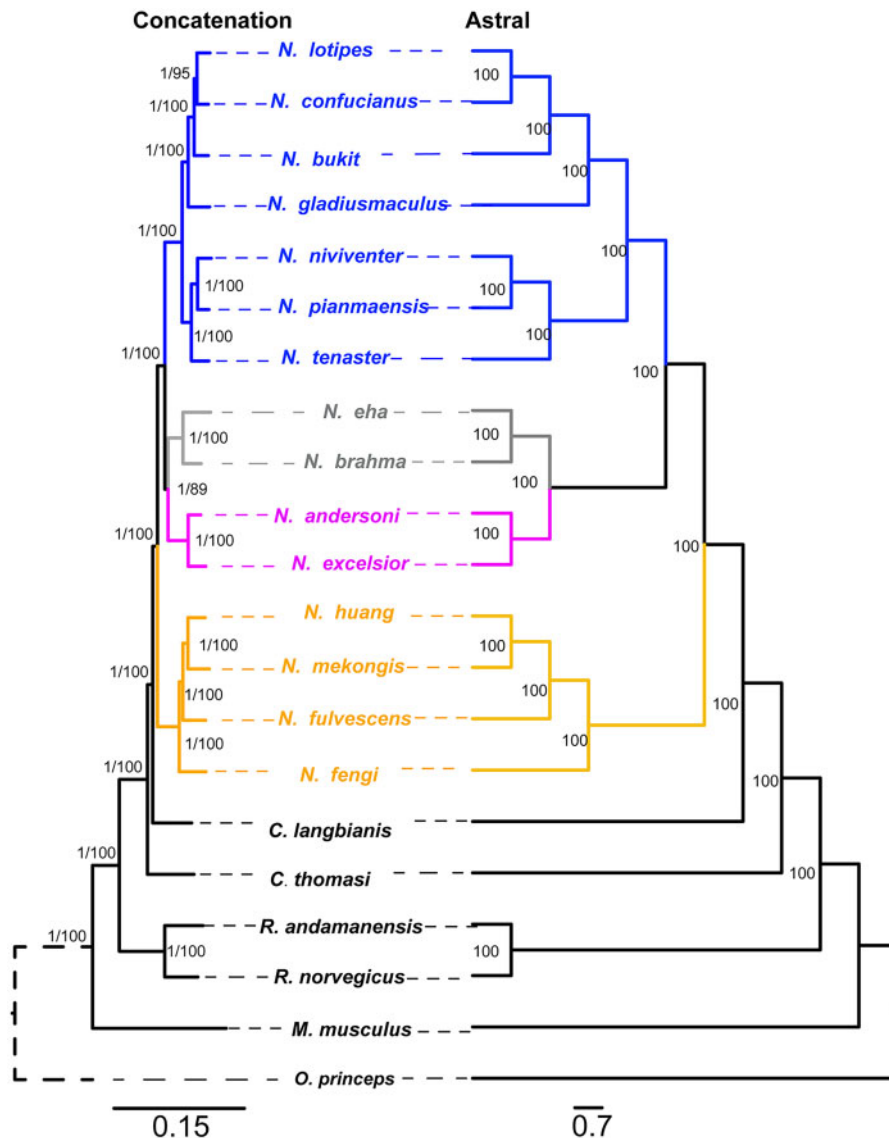


Fig. 1. Phylogeny of *Niviventer* reconstructed based on SCOs of the genome. SCOs were analyzed using the concatenation and ASTRAL methods, respectively.

China; and 4) the *N. fulvescens* species complex (NFSC, *N. hinpoon*, *N. rapit*, *N. cremoriventer*, *N. huang*, *N. fengi*, *N. fulvescens*, etc.), extending farther south in Asia, with a distribution in Southeast and Central China (Lu et al. 2015; Zhang, He, et al. 2016).

Phylogenetic networks reconstructed using the Autumn algorithm (Huson and Linz 2018) recovered three networks, each of them showing three hybridization events (fig. 2A–C). Hybridization was inferred 1) between the ancestors of NESC and NFSC; 2) the common ancestor of *N. huang* and *N. mekongis* with *N. fulvescens*; 3) the common ancestor of *N. huang* and *N. mekongis* with *N. fengi* to generate *N. fulvescens*; 4) the common ancestor of NESC with a clade of NNSC (*N. pianmaensis* and *N. niviventer*) to generate NASC; 5) as well as between *N. fulvescens* and *N. fengi*. Inferring the species network using maximum pseudolikelihood (Yu and Nakhleh 2015) and Bayesian inference (Wen et al. 2016) in Phylonet identified four hybridizations, which not only occurred

between the ancestors of *Niviventer*, but also between *Niviventer* and *Chiromyscus* (fig. 2D and E). Analyses in Phylonetworks (Solís-Lemus et al. 2017) recognized four hybridizations (fig. 2F): NNSC proposed as a hybrid of the common ancestor of NASC and NESC with the common ancestor of *N. huang* and *N. mekongis*. Inheritance values (γ) for the former is 0.969, whereas that of the latter is 0.031. The common ancestor of NESC and NASC hybridized with the ancestor of NASC ($\gamma = 0.025, 0.075$, respectively). The ancestor of *N. niviventer* and *N. pianmaensis* hybridized with the ancestor of *N. tenaster* ($\gamma = 0.857, 0.143$, respectively), *N. confucianus* hybridized with *N. lotipes* ($\gamma = 0.965, 0.035$, respectively).

The divergence time of *Niviventer* based on MTG was dated to the late Miocene, at ~ 6.49 – 4.99 Ma (supplementary fig. 2B, Supplementary Material online). The split of NESC and NFSC was dated to 6.05–4.63 Ma, and the split of NASC and NNSC was dated to 5.78–4.42 Ma. The divergence time of

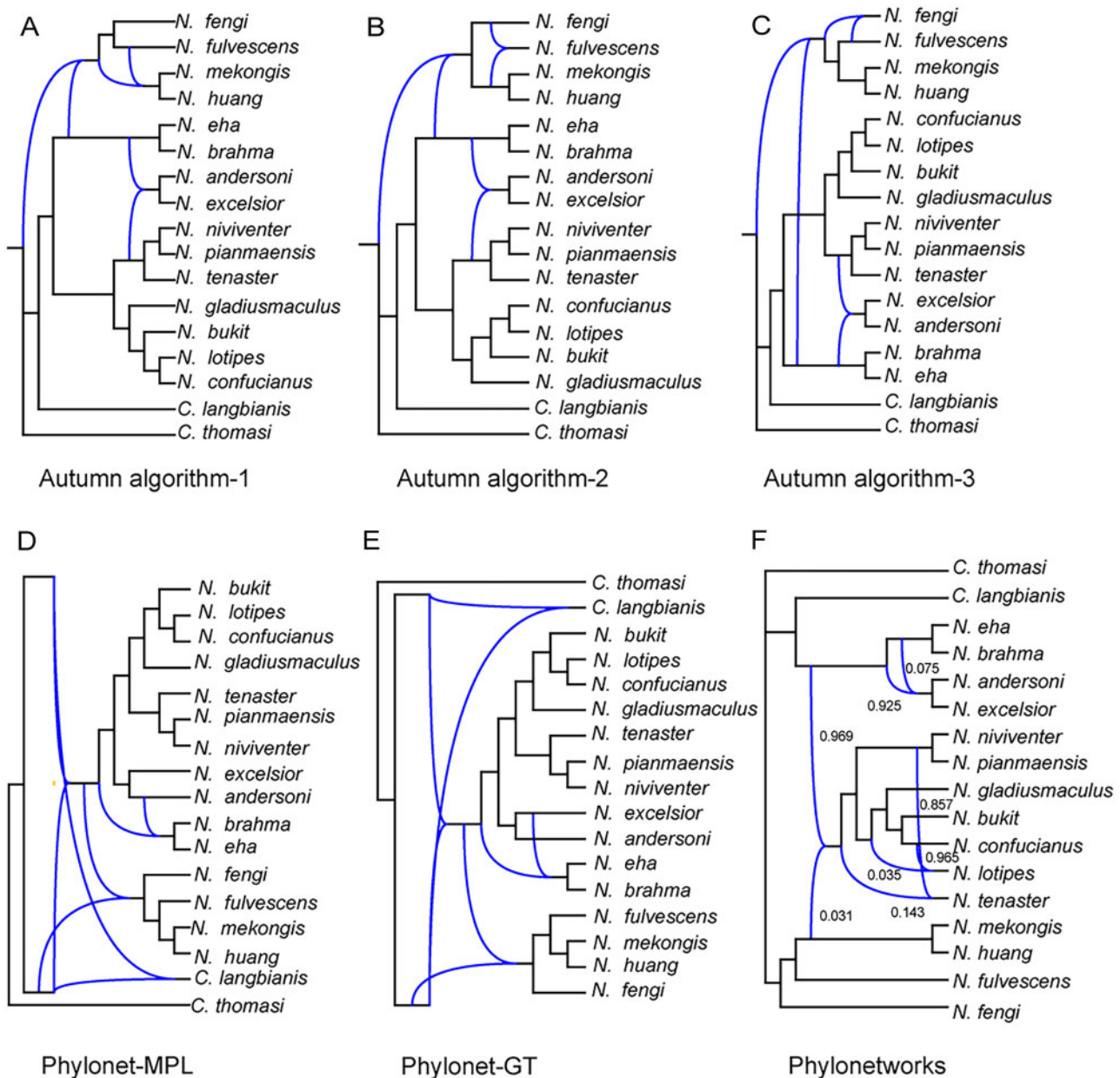


Fig. 2. Phylonetworks inferred using four different methods. Analyses were based on the best gene trees reconstructed using maximum likelihood in RaxML.

Niviventer based on SCOs of the genome was dated to 5.88–4.60 Ma (fig. 3C). The split of NFSC was dated to 3.16–2.46 Ma. Divergence of NESG and NASG was dated to 4.36–3.41 Ma. Divergence of NNSG was dated to 3.08–2.4 Ma. These results highlighted a rapid speciation of *Niviventer* since the late Miocene.

Biogeographic history reconstruction of *Niviventer* using statistical Dispersal-Vicariance Analysis (S-DIVA) and Bayesian Binary MCMC (BBM) by the trees generated from MTG and SCOs revealed its origin on the southeastern QHTP (fig. 4A–D). Four major geographical scenarios were detected in the evolution of these animals: 1) NESG remained on the southeastern QHTP and in western Yunnan and did not shift its range; 2) NASG expanded to the high mountains surrounding the southeastern and eastern QHTP to the

Qingling and Wuling mountainous region in China; 3) NNSG dispersed to the southeast, center and north of China and mountainous regions in Southeast Asia; and 4) NFSC dispersed to Southeast Asia and southeastern China. Reconstruction of elevational evolutionary history of this genus using the tree generated from BEAST analyses based on the whole-genome data revealed this taxon probably originated at ~2,100 m (supplementary fig. 3, Supplementary Material online).

Demographic History and Range Shifts of *Niviventer*

Tajima's *D*, Fu and Li's *D*, Fu and Li's *F*, and Fu *F*s tests and mismatch tests showed significant population size increases in *N. confucianus*, *N. lotipes*, *N. mekongis*, *N. niviventer*, and *N. huang* (supplementary table 4 and fig. 4, Supplementary

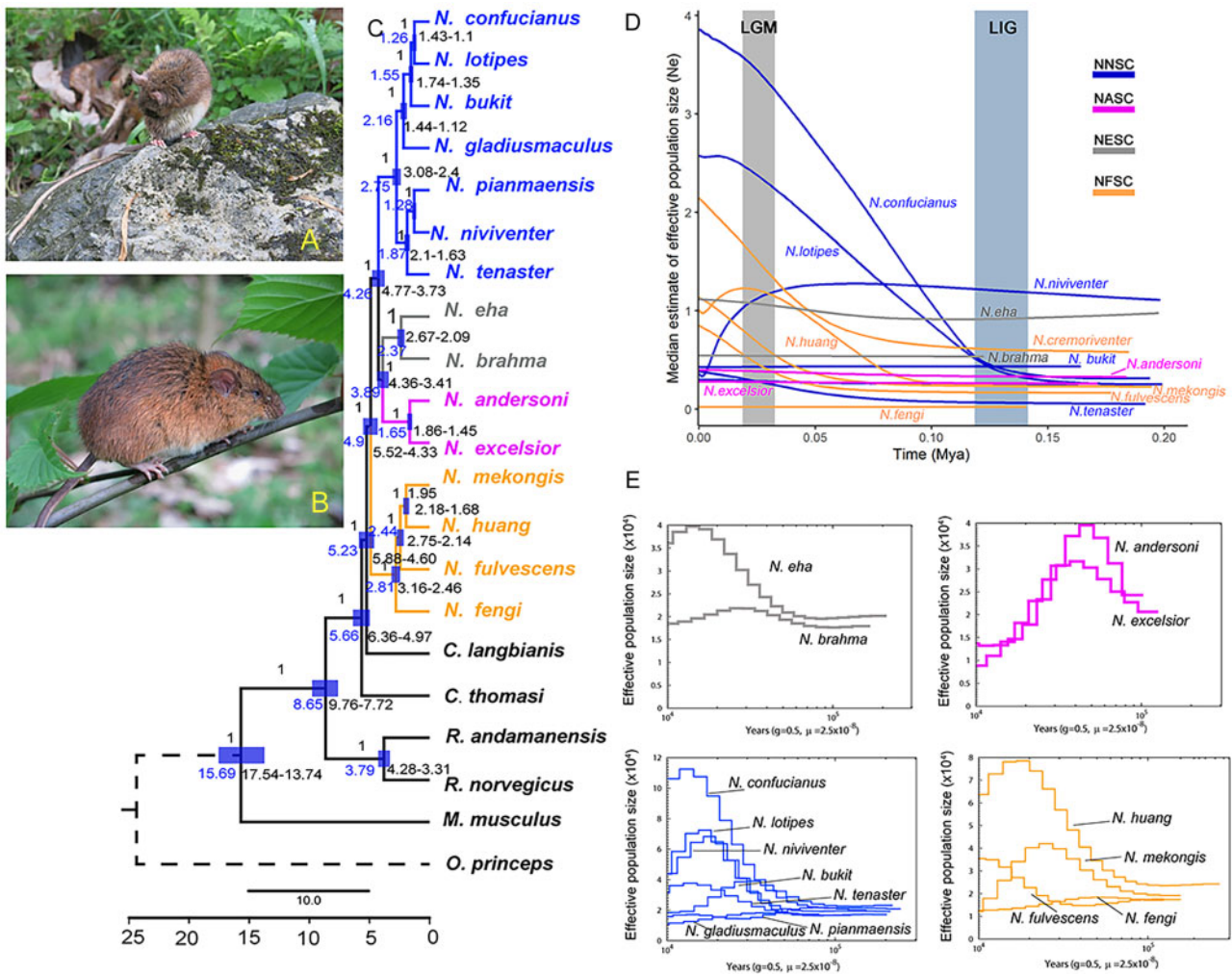


FIG. 3. Profiles, divergence time, and demographic history of *Niviventer*. (A) *N. andersoni*. (B) *N. huang*. Photographer: Deyan Ge. (C) Divergence time of *Niviventer* inferred using SNP sites of all SCOs. (D–E) Demographic history of species within *Niviventer* inferred based on CYTB using EBS (D) and PSMC based on the whole-genome data (E).

Material online). Inference of demographic history from variation in mitochondrial *CYTB* using Extended Bayesian Skyline Plots (EBS) in BEAST (Drummond and Rambaut 2007) revealed marked population size increases for the same five species, all of which inhabit wider ranges when compared with their congeners (supplementary fig. 1, Supplementary Material online). Clear population size increases were also evident in *N. tenaster*, *N. fulvescens*, and *N. eha*. The first two species are distributed in the mountainous region in southeast Asia and in southeast of the QHTP, whereas *N. eha* occurs on the QHTP at high elevations. There was little change in the population sizes of middle to alpine mountain species, including *N. fengi*, *N. brahma*, and *N. bukit*. *Niviventer andersoni* and *N. excelsior* also showed a relative stable population size, but dramatic population size decreases were shown using the autosomal genome data. *Niviventer huang* in Southeast China showed initial population size increase, but its population size dramatically decreased in the last 0.025 Ma (fig. 3D and supplementary fig. 5, Supplementary Material online). *Niviventer niviventer* demonstrated a trend

of decreasing population size since 0.05 Ma. The analysis of demographic history from heterozygous sites in the nuclear genome using the pairwise sequential Markovian coalescent (PSMC) model (Li and Durbin 2011) was generally consistent with the above conclusions (fig. 3E). We identified population size increases in *N. confucianus*, *N. lotipes*, *N. bukit*, *N. eha*, and *N. mekongis*, population size decreases in *N. andersoni*, *N. excelsior*, *N. niviventer*, and *N. fulvescens*; and population size stability in *N. brahma*, *N. fengi*, and *N. pianmaensis*, the last of which were confined to small regions on the southeastern QHTP (fig. 3E).

Genes under Positive Selection

Genome scanning by PosiGene with validation in PAML revealed *N. eha* has the largest number of positively selected genes among the four species complexes based on the present data sets (Table 1, supplementary table 5, Supplementary Material online). Bayesian inference using these genes revealed clear topological inconsistency when compared with the species tree reconstructed using the

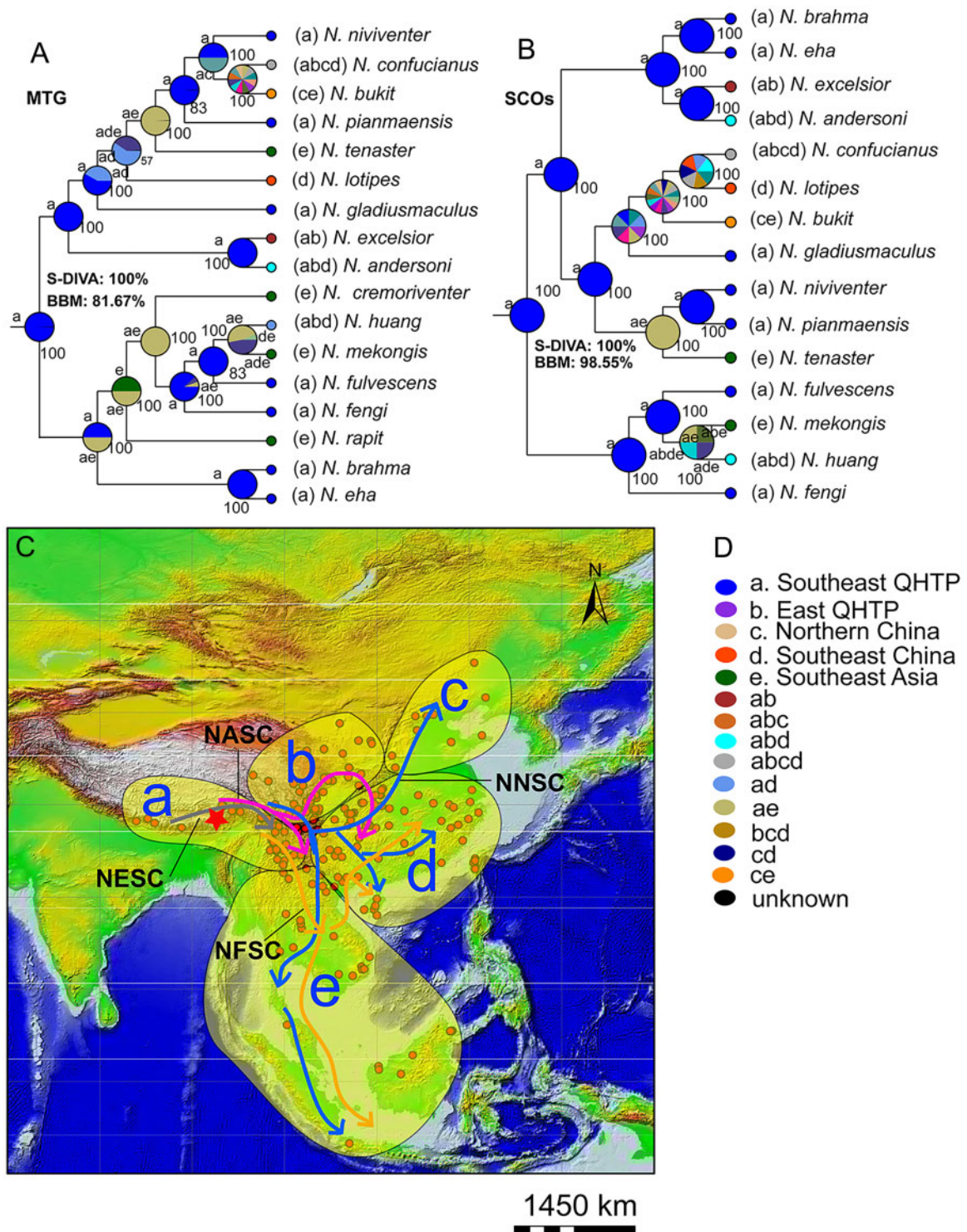


Fig. 4. Phylogeographic evolution of *Niviventer*. MTG (A) and SCOs of the whole genome (B) were analyzed separately. Both S-DIVA and BBM methods supported an origination history of *Niviventer* from southeast QHTP.

whole data set of SCOs (fig. 5), which implies adaptive evolution in these genes.

About 17 genes of *N. eha* showed a P value <0.05 (supplementary table 5, Supplementary Material online). These included four genes from the olfactory receptors (*OLR141*, *OLR1658*, *OLR224*, *OLR590*), two genes from the taste receptors (*TAS2R114*, *TAS2R118*), coiled-coil domain containing 73

(*CCDC73*), cytochrome P450 family 8 subfamily B member 1 (*CYP8B1*), dopamine receptor D5 (*DRD5*), fibroblast growth factor 22 (*FGF22*), G protein-coupled estrogen receptor 1 (*GPER1*), heat shock factor 1 (*HSF1*), kinesin family member 20 A (*KIF20A*), large tumor suppressor kinase 2 (*LATS2*), protocadherin beta 2 (*PCDHB2*), protein tyrosine phosphatase domain containing 1 (*PTPDC1*), and SET domain containing

Table 1. Positively Selected Genes Detected in *Niviventer brahma*, *N. eha*, and *N. fengi*.

Target Species	Genes	Homologous Transcript in <i>Rattus norvegicus</i>	Number of Species Selected by PosiGene	P Value Raw	Adjusted P Value Resulted in PosiGene	Number of Species Included in Final Evaluation in PAML	P Value Resulted in CODEML in PAML	FDR
<i>Niviventer brahma</i>	HOXC8	NM001177326	4	<0.0001	<0.0001	16	0.0001	0.0001
<i>Niviventer eha</i>	OLR141	NM001001274	3	<0.0001	<0.0001	6	<0.0001	0.0006
<i>Niviventer eha</i>	OLR1658	NM001000105	4	0.0048	0.0048	11	<0.0001	0.0006
<i>Niviventer eha</i>	PTPDC1	XM006253700	3	<0.0001	<0.0001	13	<0.0001	0.0006
<i>Niviventer eha</i>	KIF20A	NM001108426	3	0.0001	0.0001	18	0.0002	0.0009
<i>Niviventer eha</i>	CCDC73	XM006224541	6	<0.0001	<0.0001	14	0.0012	0.0041
<i>Niviventer eha</i>	HSF1	NM024393	4	0.0014	0.0014	17	0.0035	0.0097
<i>Niviventer eha</i>	OLR224	NM001000553	5	0.0077	0.0077	20	0.004	0.0097
<i>Niviventer eha</i>	TAS2R118	NM023994	5	0.0001	0.0001	19	0.0054	0.0115
<i>Niviventer eha</i>	SETD2	XM008766632	3	0.0036	0.0036	15	0.0149	0.0269
<i>Niviventer eha</i>	OLR590	NM001000658	6	0.0175	0.0175	16	0.0158	0.0268
<i>Niviventer eha</i>	GPFR1	NM133573	3	0.0135	0.0135	19	0.0179	0.0277
<i>Niviventer eha</i>	DRD5	NM012768	5	0.0036	0.0036	19	0.021	0.0298
<i>Niviventer eha</i>	LATS2	XM008770748	3	0.0143	0.0143	14	0.028	0.0338
<i>Niviventer eha</i>	PCDHB2	NM001109123	3	0.0077	0.0077	8	0.0291	0.0338
<i>Niviventer eha</i>	TAS2R114	NM023996	3	0.008	0.008	3	0.0298	0.0338
<i>Niviventer eha</i>	CYP8B1	NM031241	3	0.0045	0.0045	19	0.0358	0.038
<i>Niviventer eha</i>	FGF22	NM130751	5	0.0463	0.0463	20	0.0423	0.0423
<i>Niviventer fengi</i>	KLK9	NM001106253	4	<0.0001	<0.0001	12	<0.0001	0.006
<i>Niviventer fengi</i>	FOXD2	XM0233422	3	0.0004	0.00035	19	0.0011	0.033
<i>Niviventer fengi</i>	CYP27B1	XM008765374	4	<0.0001	<0.0001	14	0.0393	0.0428
<i>Niviventer fengi</i>	TAF7L	NM001135877	4	0.0356	0.0356	9	0.0415	0.0428
<i>Niviventer fengi</i>	ERCC6L	NM001098674	4	0.0114	0.0114	12	0.0428	0.0428

NOTE.—The full list of PGS selected by PosiGene is given in [supplementary table 6, Supplementary Material](#) online.

2, histone lysine methyltransferase (*SETD2*, [fig. 6](#) and [supplementary fig. 7, Supplementary Material](#) online).

Five genes were identified as positively selected in *N. fengi*, cytochrome P450, family 27, subfamily b, polypeptide 1 (*CYP27B1*), forkhead box D2 (*FOXD2*), TATA-box binding protein associated factor 7-like (*TAF7L*), ERCC excision repair 6 like, spindle assembly checkpoint helicase (*ERCC6L*), and kallikrein related-peptidase 9 (*KLK9*). One gene, homeobox C8 (*HOXC8*), was identified as positively selected in *N. brahma* ([supplementary table 5, Supplementary Material](#) online).

GO enrichment analyses of biological processes revealed *N. eha* had 24 significantly enriched functions ([supplementary table 6, Supplementary Material](#) online). G protein-coupled receptor signaling pathway, sensory perception of chemical stimulus, and cell cycle process ranked as the top three enriched functional categories. Some of these positively selected genes, for example, *SETD2* ([fig. 6](#)), *HIF1*, *LATS2* were involved in multiple biological processes, which means they are pleiotropic genes and playing diverse roles in local adaptation. However, *N. fengi* and *N. brahma* have too few genes identified as under positively selection, and no significant enriched biological pathway was detected in these two species based on the present data set.

Niche Evolution in *Niviventer*

Models of the effects of climate change on species distributions using ecological niche models (ENMs) revealed marked overall temporal range shifts in *Niviventer* species ([fig. 7](#) and [supplementary fig. 7, Supplementary Material](#) online). The transition from Last Interglacial (LIG) to the

cold and arid Last Glacial Maximum (LGM) increased the suitable areas for white-bellied rats by 43%, whereas the transition from the LGM to warmer contemporary conditions decreased the area by 39%. Thirty years from now, suitable habitats are expected to expand southward in low elevations by ~9% ([supplementary table 7, Supplementary Material](#) online). Nevertheless, idiosyncratic responses to range shifts over time were observed across species ([fig. 7](#)). Most species showed alternating cycles of range expansion and contraction from the LIG to future scenarios (e.g., *N. cremoriventer*, *N. fulvescens*, *N. mekongis*, and *N. rapit*), whereas a few exhibited a continued decline (*N. andersoni*) or expansion (*N. huang*) of suitable areas through the Quaternary. The suitable area of nine species will be reduced by up to 66% ([fig. 7A](#) and [supplementary table 7, Supplementary Material](#) online), species endemic in middle to high elevation will shift upward under the future global warming, whereas those at lower elevation will expand and then the average elevational range of these species will decrease ([fig. 7A](#) and [supplementary table 7, Supplementary Material](#) online). Future climate change will mostly negatively affect species with subtropical and temperate distributions and those that inhabit high elevations. Conversely, for five species, the ongoing global warming will lead to an expansion of suitable habitats of up to 58% ([fig. 7](#)). These species mainly show a tropical distribution in Southeast Asia and in the southern portion of QHTP or inhabit a wide elevation range in subtropical zones, reflecting their adaptation to contrasting climatic conditions. Notably, *N. eha* will increase its distribution

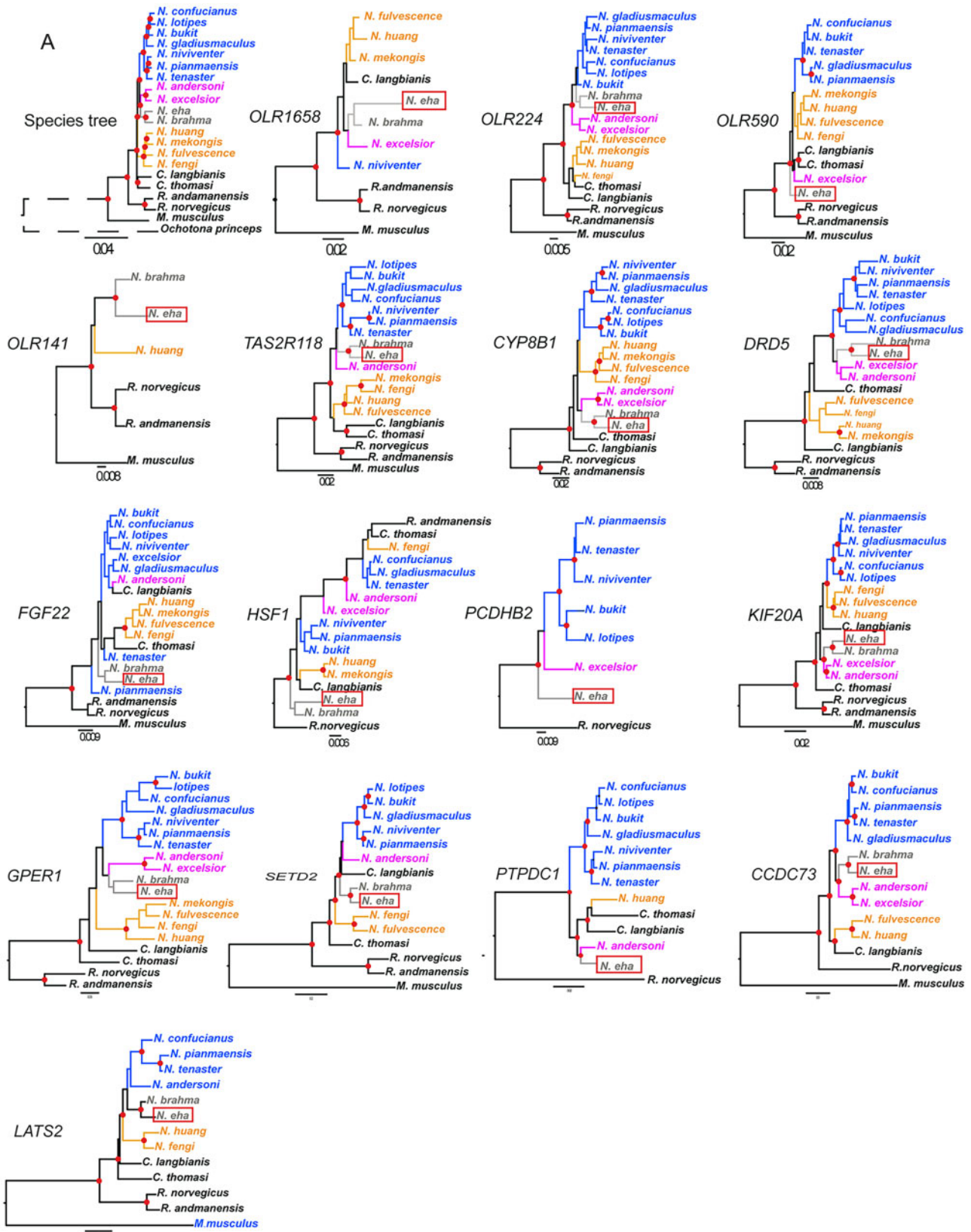


FIG. 5. Species tree of *Niventer* compared with gene tree of positively selected genes. (A) Species tree, gene trees of OLR1658, OLR224, OLR590, OLR141, TAS2R118, CYP8B1, DRD5, FGF22, HSF1, PCDHB2, KIF20A, GPER1, SETD2, PTPDC1, CCDC73, LATS2. These genes are positively selected in *N. eha*. (B) Gene tree of TAF71, LOC100909462, KLK9, ERCC6L, FOXD2, HOXC8. The first five of them are positively selected in *N. fengi*, and the last one of them was positively selected in *N. brahma*. Node marked with red points with posterior probabilities (pp) = 1. Genes present in less than five species were not used to reconstruct gene tree.

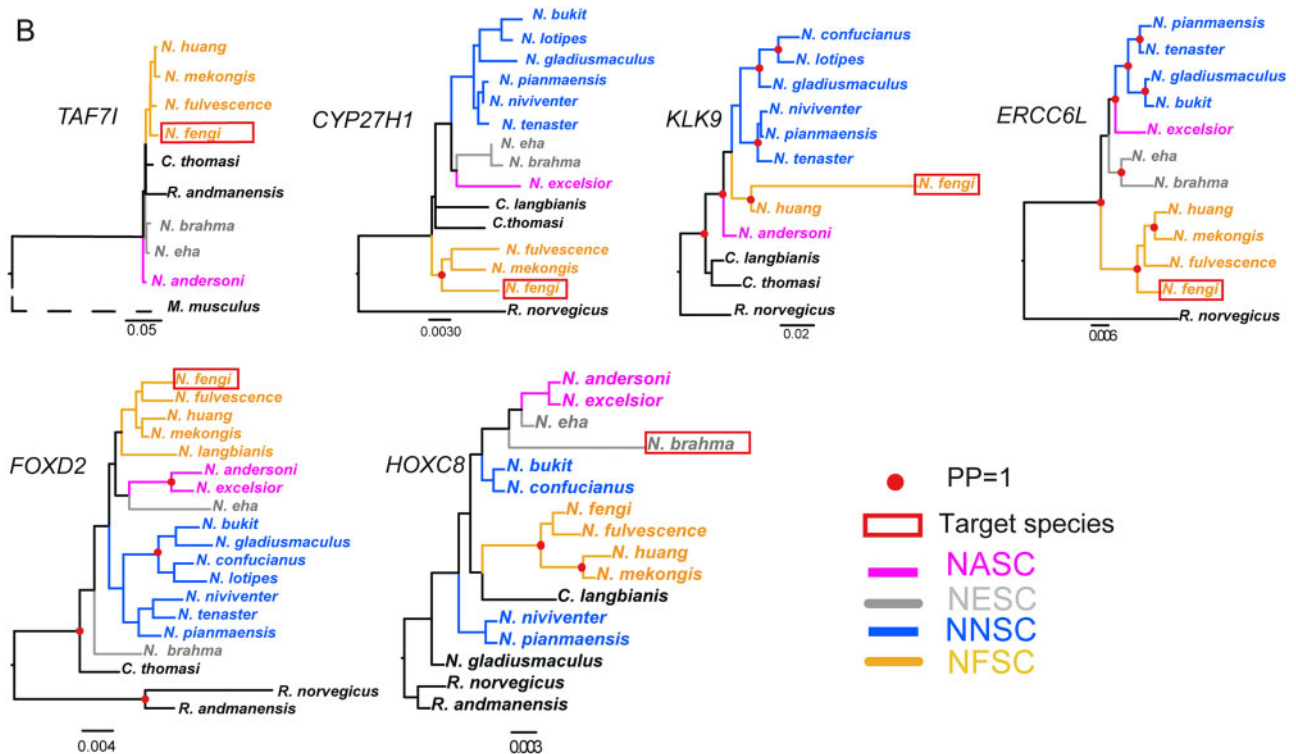


Fig. 5. continued

toward the QHTP, while reducing its range in low elevation areas.

The age-range correlation analysis showed a marked range overlap between sister species in recent nodes (supplementary fig. 8, Supplementary Material online), and a negative but nonsignificant relationship between range overlap and phylogenetic age (intercept 0.476, $P = 0.34$; supplementary fig. 8A, Supplementary Material online). When reconstructing the climatic tolerance of species, we detected one major split in the early stages of *Niviventer* evolutionary history, resulting in a tropical environment-adapted clade formed by the NFSC and temperate environment-adapted clades formed by the remaining species (supplementary fig. 8C, Supplementary Material online). Within the NFSC, three species (*N. huang*, *N. fulvescens*, and *N. mekongis*) later converged toward a more temperate climate. Interestingly, four of the five species predicted to undergo range expansions in the future belong to this tropical environment-adapted clade.

Discussion

Out of Tibet: The Geographical Evolution of *Niviventer*

The QHTP is a young and large high-altitude plateau. Prior to the uplift in the early to the middle Miocene, this region was characterized by warm and humid environments (Zhang, Ao, et al. 2016; Li, Zhou, et al. 2020), as evidenced by warm-climate C_4 grasses present as a significant dietary component of ancient herbivores on the QHTP (Wang XM, Wang Y, et al. 2015). Until recently, the QHTP harbored many large mammals that went extinct in the late Quaternary, and these

species likely began shifting their ranges away from Tibet beginning with cooling at the end of the Pliocene (Deng et al. 2011; Wang et al. 2016). Biogeographic shifts out of Tibet have been hypothesized for several large mammalian lineages, including an ancestral woolly rhinoceros, *Coelodonta thibetana* (Wang et al. 2013; Wang XM, Wang Y, et al. 2015); the early sheep, *Protovis himalayensis* (Wang et al. 2016); a hypercarnivorous canid, *Sinicuon cf. dubius* (Wang, Li, et al. 2015); a pantherine cat, *Panthera blytheae* (Li et al. 2014); the running hyena, *Chasmaporthetes gangsriensis* (Tseng et al. 2013); and an ancient Arctic fox, *Vulpes qiuzhudingi* (Wang et al. 2014).

The out-of-Tibet concept postulates that the uplifting QHTP acted as a “cradle of evolution” for cold-loving ice age mammals (Wang et al. 2014). Small mammals are excellent indicators for understanding the response of animals to regional environmental changes and ecosystem health. They show high diversity with verifiable geographical evolutionary histories, and thus can serve as models for studying regional biodiversity and faunal changes (Leis et al. 2008; Barnosky et al. 2012). For example, pikas (*Ochotona* spp.) as the keystone species of the QHTP (Smith and Foggini 1999; Lai and Smith 2003) are good examples of small mammals that originated on the QHTP and dispersed to Eurasia, Africa, and North America. However, pikas have experienced dramatic extinction and contraction in a wide range outside of the QHTP (Ge et al. 2013; Wang et al. 2020). They therefore represent relic mammalian taxa that were adapted to a cold environment before leaving the QHTP but now show a trend of retracting to the QHTP under global warming.

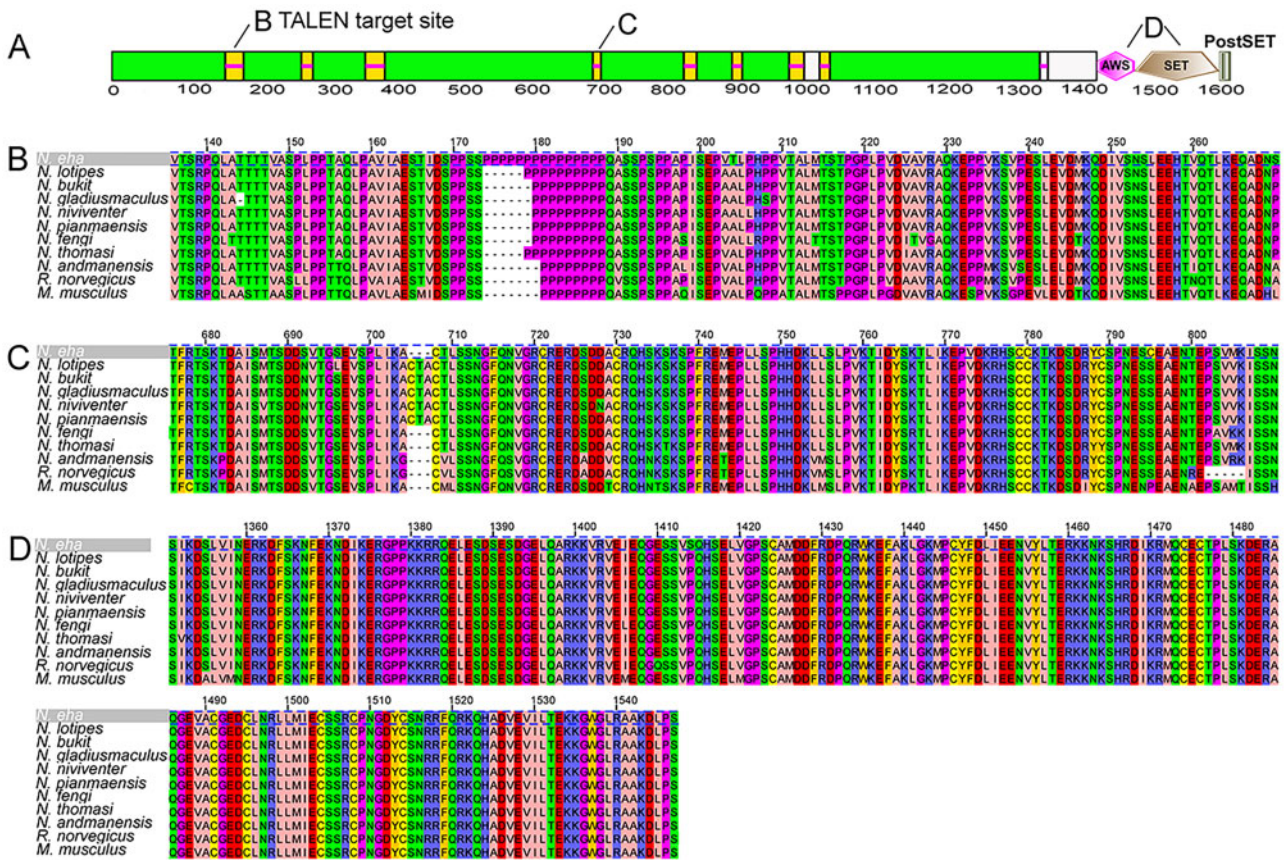


FIG. 6. Mutation in partial protein sequence of *SETD2*. (A) Protein structure predicted in SMART, and the location of annotated domain from 1 to 1,600. (B) 136–270 of *SETD2*. (C) 676–810 of *SETD2*. (D) 1,350–1,547 of *SETD2*.

In this study, we inferred the geographical origin of the genus *Niviventer* on the southeastern QHTP. The NASC, NNSC, and NFSC lineages of this genus present good examples of extant mammals that adapted to temperate and tropical environments after leaving the QHTP. However, the NESc, the earliest diverging clade within *Niviventer*, is confined to the QHTP. These results indicate that the QHTP not only is the cradle for cold-loving species but also initiates the diversification of mammalian taxa, which now disperse to tropical and temperate regions.

Adaptive Genetic Evolution in *Niviventer*

Positive natural selection, or the tendency of beneficial traits to increase in prevalence in a species, is the driving force behind adaptive evolution. Genome level scans identified *N. eha* as having the largest number of positively selected genes among *Niviventer* species, here interpreted as adaptive genetic changes associated with the high-altitude environment on QHTP. Five positively selected genes were identified in *N. fengi*, also present at high altitude but endemic to the Jilong Valley in the southeastern QHTP where it is sympatric with the much more widely distributed *N. eha*. The range expansion toward the QHTP and the population size increase of *N. eha* highlights its adaptation to the high elevations, likely via the fixation of many new advantageous alleles, particularly those involved in olfactory sensitivity, taste, and tumor suppression. Small population size can be assumed to have

resulted in the rapid fixation of these advantageous alleles, as currently evidenced by *N. eha*.

The expansion of *N. eha* within the QHTP likely coincided with rapid genetic modification in response to global warming. Surprisingly, the greatest number of genes under selection was in the olfactory receptor genes (*OLR141*, *OLR224*, *OLR590*, *OLR1658*), the largest gene family in the mammalian genome (Buck and Axel 1991). The types of genes detected in these scans provide insight into the adaptations that coincide with the high-altitude habitats. The ability of this species to distinguish food resources and to discover predators timely influences their survival and reproductive capacity. Reduction of olfactory sensitivity during hypoxia is a common symptom of altitude sickness. Living on the QHTP likely has some selective regime affecting olfaction of *N. eha*. Moreover, genes of taste receptor (*TAS2R114*, *TAS2R118*) are under positive selection, which provide additional evidence that adaptations to an environment where olfaction and taste play an important role for survival, more so than in middle or low altitude habitats (Lossow et al. 2016). However, high-quality genome assemblies and annotations for these species are still needed for detailed study on the evolution of these genes due to their large number and high similarity.

A recent study revealed a high risk of cancer occurrence as a result of evolutionary adaptations to cold environments (Voskarides 2018). Consistent with this finding, several positively selected genes of *N. eha* regulate important biological

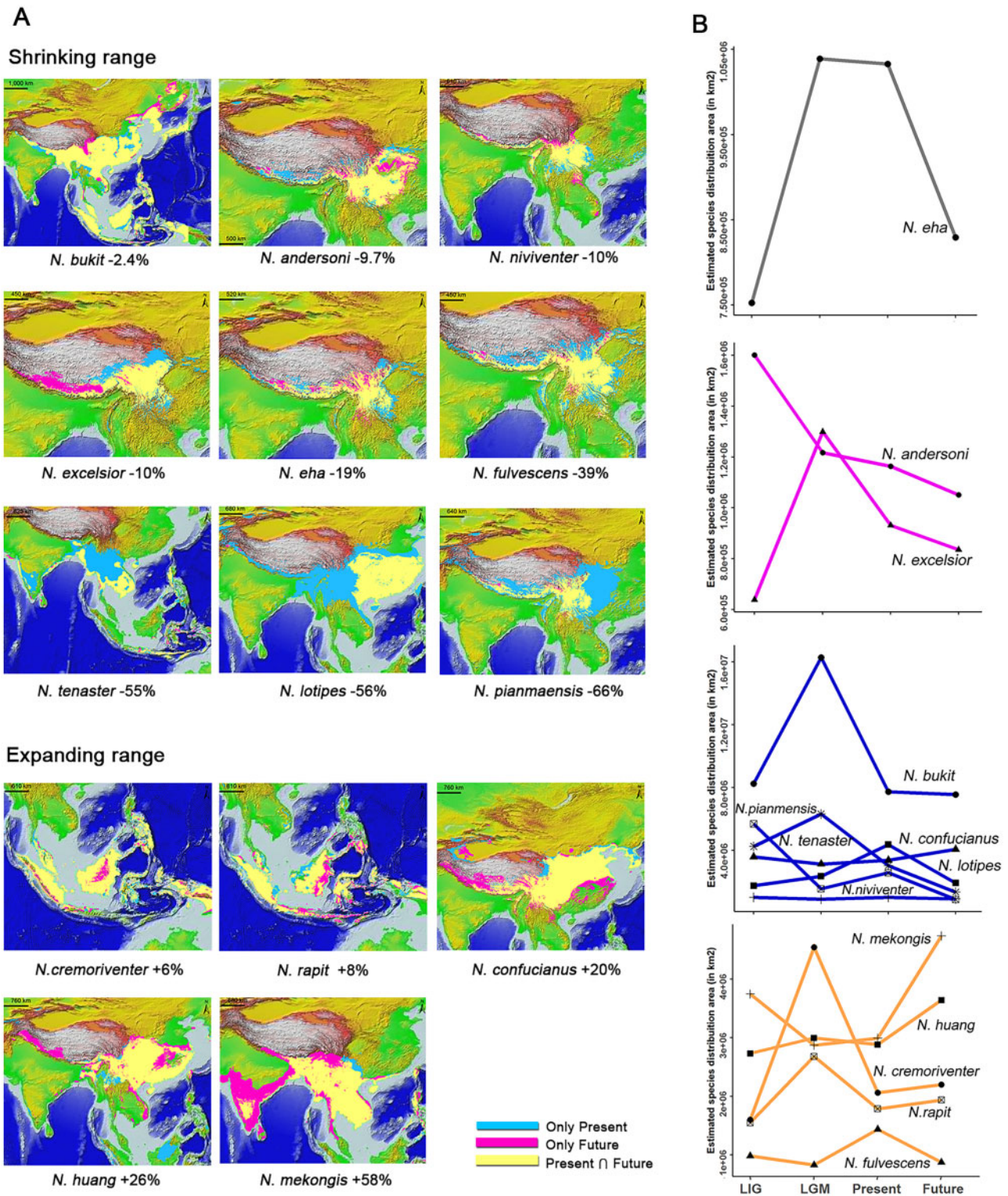


FIG. 7. Temporal shifts in suitability areas of *Niviventer* species. (A) Present (blue) and future (pink) modeled distributions overlapped, showing the intersection area (yellow). (B) Trends in suitability area shifts through LIG, LGM, present and future, the color of lines represent different species complexes, which are same as figures 1 and 3.

processes that may be involved in suppression of cancer occurrence. *SETD2* acts as an epigenetic modifier with tumor suppressor functionality (Li et al. 2016), and also regulates the maternal epigenome, genomic imprinting, and embryonic development (Xu et al. 2019). *SETD2* shows high level of

nucleotide variation in *Niviventer*, particularly in the TALEN target sites region, whereas the main functional domains in AWS (associated with SET) and SET are highly conservative (fig. 6). *DRD5* inhibits tumor growth (Leng et al. 2017). *LATS2* is a core member of the Hippo pathway that regulates organ

size (Aylon et al. 2016). *FGF22* plays important roles in regulating impairment of ribbon synapses (Li, He, et al. 2020), as well as cutaneous development and repair (Beyer et al. 2003). *PCDHB2* is involved in cell adhesion (Carter et al. 2010). Moreover, *KIF20A* regulates the division modes of neural progenitor cells during cortical development (Geng et al. 2018). *HSF1* was discovered as a transcriptional response to elevated temperature shock, and also regulates mevalonate and cholesterol biosynthesis pathways (Li et al. 2017). *CYP8B1* catalyzes cholic acid synthesis in the liver and then regulates fat absorption (Jahan and Chiang 2005). *GPER1* is believed to be involved in emotional and cognitive functions and stress control (Jahan and Chiang 2005). Molecular variation of these genes in *N. eha* likely enhances its ability to cope with recent environmental changes on the QHTP.

The positively selected genes identified in *N. fengi* are different from *N. eha* even though two species slightly overlap in the southeastern QHTP. Among these genes, *FOXD2* is critical to control of the cell cycle and metabolism (Johansson et al. 2003). *ERCC6L* is a DNA helicase. It is involved in cell proliferation and associated with embryonic development and in maintaining growth (Yin et al. 2011). Kallikrein-related peptidases, including *KLK9*, have been reported to possess functions in innate immunity and inflammation (Filippou et al. 2020). For the only one identified positively selected gene of *N. brahma*, *HOXC8* is a homeobox gene family member, which is essential for growth and differentiation; over expression of *HOXC8* reduces cell adhesion and concomitant cell migration, and regulates tumor growth (Ruthala et al. 2011).

In contrast, species present with mostly midaltitude ranges, even if extended into the high elevation, show no genes under positive selection, as is evident in *N. niviventer*, *N. fulvescens*, *N. andersoni*, *N. pianmaensis*, *N. gladiusmaculus*, and *N. excelsior*. This is despite some obvious morphological adaptations, for example, the divergent external and cranial dental morphologies of *N. andersoni*. This species is the largest species of *Niviventer*, but we did not detect positively selected genes in the nuclear genome of this species. In contrast, *N. eha* is the smallest species, yet showed the largest number of positively selected genes. This suggests that genetic adaptive changes detected in genome scans do not primarily detect the kind of changes leading to morphological adaptive evolution, but rather reveal physiological (growth and cell proliferation) and sensorial (taste, olfaction) functions. The ease with which genomes scans of the kind used here can be implemented, adaptive radiations of a wide range of species can be investigated to link the signatures of genomic selection to specific adaptive shifts in life style, environmental conditions, morphological features or other traits, as well as demographic changes that may be needed for the rapid fixation of adaptive mutations.

Ecological Differentiation and Demographic History of *Niviventer*

In the genus *Niviventer* we can distinguish two major lineages separating the mostly temperate and tropical NASC, NNSC, and NFSC lineages from the early diverging NESC complex confined to the cold conditions of the QHTP. These apparent

climatic adaptations could be linked to idiosyncratic responses to temporal range shifts in *Niviventer* species. Most species in the tropical environment-adapted NFSC clade are expected to expand their range in the future under global warming (Dallmeyer et al. 2017). Likewise, the habitat generalist, *N. confucianus* will experience a range increase of 20%, likely related to increasing vegetation in central to northern China (Li, Chen, et al. 2015). *Niviventer eha*, which occupies the highest elevations among *Niviventer* species, displayed a clear trend of expansion in terms of both population size and potential range toward higher areas of the QHTP. This pattern is different from that of other species restricted to a small range on the southeastern QHTP and in western Yunnan. For example, *N. brahma* (sister species of *N. eha*), *N. pianmaensis*, and *N. fengi* are confined to small regions located on the southeastern QHTP, the most complex terrain shaped by deep valleys, rivers, and high mountains, which likely prohibit their range expansion. Future climate change will drive these species to move to higher elevations (supplementary table 7, Supplementary Material online).

Ecological differentiation analyses suggest that either sympatric speciation plays an important role in *Niviventer* diversification or the spatial overlap may represent climate segregation along mountain slopes. For example, although there is a very high degree of range overlap among species in NNSC (supplementary fig. 1, Supplementary Material online), we detected marked disparities in climatic tolerance, especially in temperature-related traits, such as the presence of spines on the skin, suggesting that the species have adapted to distinct conditions along mountain slopes.

Inferences from climatic envelope modeling were largely consistent with demographic population models from mitochondrial markers and genome data. *Niviventer confucianus* showed the most prominent population size increases (fig. 3), probably due to its high tolerance of habitat variation. This species can be considered native “weedy” species that have recently risen in dominance (Rowe and Terry 2014). Interestingly, we did not identify significant positively selected genes in *N. confucianus*. Together with *N. eha*, which is expanding in population size and range toward high elevations, possibly driven by decreased predation from carnivores and competition with other herbivores, these species may threaten human health and ecosystem safety since most reports of hantavirus in *Niviventer* were from these two species (Cao et al. 2010; Lin et al. 2012; Ge et al. 2016).

Conversely, the mid-to-high elevation species *N. niviventer*, *N. andersoni*, *N. excelsior*, and *N. fulvescens* showed a trend of decreasing population size based on PSMC analysis and a decreasing in suitable future areas, which was correlated with climate warming and a gradual increase in the impact at these elevations. The population decline of *N. huang* mirrored the rapid population increase of humans in Southeast China since this species was confined to a lower elevation, where the development of agriculture and forestry accelerated the change in land usage (Shi et al. 2018).

In summary, the genus *Niviventer* originated on the QHTP, successfully dispersed from the QHTP, and adapted to

temperate and tropical regions in Asia. The NASC, NFSC, and NNSC successfully left the QHTP, but they showed different demographic histories in response to global environmental changes. Species from Southeast Asia and “weedy” species showed a clear trend of population expansion. Interestingly, *N. eha*, a wild rat living at high elevations showed clear trend of population increase. Genetic modifications of this species are mainly related to olfaction, taste, and tumor suppression. Deep-level sequencing and functional validation of these positively selected genes are needed for a more comprehensive understanding of the adaptive evolution of *Niviventer*.

Materials and Methods

Field Work and Sampling

The liver or muscle samples of rodents used in the present study were collected by the Institute of Zoology, Chinese Academy of Sciences (IOZCAS, Beijing, China); Kunming Institute of Zoology, Chinese Academy of Sciences (KMIOZCAS, Kunming, China), the National Institute for Communicable Disease Control and Prevention (ICDCP, Beijing, China); and the Zoological Institute of the Russian Academy of Sciences (ZIN, Saint Petersburg, Russia). All these samples were preserved in 95% ethanol at -40°C before extraction. Total DNA was extracted by using a Qiagen DNeasy Blood and Tissue Kit (Germany). Detailed information for molecular voucher specimens included in the present study is provided in [supplementary table 1, Supplementary Material](#) online, which includes collection locations, longitude, latitude, elevation, GenBank accessions, and museums or institute where we preserved the collected specimens. All animal specimens were collected in accordance with the policy of the animal care and use policies of each institution.

Sequencing of Mitochondrial DNA Markers

Historical collections of *Niviventer*, particularly species within the NFSC and NNSC, are easily misidentified when using morphology. To avoid such misidentification in the following analyses, we included Cytochrome b (CYTB) sequences from 1304 individuals of *Niviventer*, 117 of which were newly obtained in the present study. The CYTB sequences were amplified using the universal primers for mammals L14723 and H15915 (Irwin et al. 1991). PCR products were directly sequenced in both directions using ABI technology. Accessions and detailed collection information for these sequences are provided in [supplementary table 1, Supplementary Material](#) online.

Whole-Genome Sequencing

15 species of the genus *Niviventer*, two species of *Chiromyscus* (*C. langbianis* and *C. thomasi*), and one species of *Rattus* (*R. andamanensis*) were selected for whole-genome sequencing ([supplementary table 2, Supplementary Material](#) online). Whole-genome DNA was fragmented to an average length of 350 bp using a Covaris instrument. The fragmented DNA was end-polished, A-tailed, and ligated to Illumina sequencing adaptors using a TruSeq Nano DNA HT Sample Preparation Kit with further PCR amplification. The PCR products were

purified (AMPure XP system), and the libraries were analyzed for size distribution by an Agilent 2100 Bioanalyzer and quantified using real-time PCR. The paired-end libraries were submitted for paired-end sequencing (2×150 bp) on an Illumina HiSeq 1500 instrument. Sequencing was conducted by Novogene (Beijing, China).

Genome Data Quality Control

The raw read data of each species were tested and filtered using fastp (Chen et al. 2018), which is a fast, all-in-one pre-processor for quality control of FASTQ files. Low-quality bases with Phred score <20 were clipped from the 5' and 3' ends of reads. Adapters and low-quality and duplicated reads were filtered out. The quality of the cleaned data was measured using FASTQC (Schmieder and Edwards 2011; Patel and Jain 2012).

Genome Assembly

We used MEGAHIT 1.2.8 (Li, Liu, et al. 2015) for de novo assembly using the default settings. To evaluate genome completeness, we used BUSCO 3.0.2 (Simão et al. 2015) to estimate the percentage of expected conserved single-copy orthologs captured in our assemblies by using data for Glires as a reference (Kriventseva et al. 2019).

Phylogenetic Reconstruction

We established three data sets with which to reconstruct the phylogeny of *Niviventer* based on genome level data sets: 1) CYTB sequences of 1331 individuals by including outgroup taxa; 2) the complete MTG of 23 species, including 17 *Niviventer* species; and 3) the concatenated data sets of SCOs extracted from the whole-genome sequencing data, 15 of which belonged to *Niviventer*, with six outgroup species: *C. thomasi*, *C. langbianis*, *R. andamanensis*, *R. norvegicus*, *M. musculus*, and *Ochotona princeps*.

We appended the newly obtained CYTB sequences with those of previous studies, and aligned these sequences in MUSCLE 3.8.31 (Edgar 2004). We selected the best nucleotide substitution models using PartitionFinder 2.1.1 (Lanfear et al. 2017), with the three codon positions of CYTB split into different partitions. We performed Bayesian inferences using 8,000,000 generations with four independent runs in MrBayes 3.2.7 (Ronquist et al. 2012). We summarized the tree by discarding the first 25% of trees as burn-in.

To reconstruct the phylogeny based on the MTG, we used NOVOPlasty (Dierckx et al. 2017) to assemble the MTG from the whole clean reads. The MTG of *R. norvegicus* (KM577634) was used as a reference. We used MitoZ 2.4 (Meng et al. 2019) to annotate these sequences. Whole mitochondrial DNA sequences with annotation information from 18 species were submitted to GenBank under accession numbers MW193727–MW193744, and detailed information for these data is provided in [supplementary table 2, Supplementary Material](#) online.

Complete MTG sequences of *N. rapit* (KY117572) and *N. cremoriventer* (KY117573) were downloaded from GenBank. These genomic data from GenBank were annotated with MitoZ. Thirteen protein-coding sequences from newly

sequenced taxa and those downloaded from GenBank were aligned using MUSCLE (Edgar 2004) and concatenated together. We used PartitionFinder 3.8.31 (Lanfear et al. 2017) to select the most appropriate partition sets for this data set. We performed Bayesian inferences as above.

To extract single-copy orthologs from the whole-genome data, we used the assemblies from MEGAHIT as the input file. The SCOs of Glires provided by OrthoDB (Kriventseva et al. 2019) were used as a reference database. We aligned the protein sequence from each of the reference species to that from each newly assembled species by TblastN of the BLAST (Altschul et al. 1990), and all coding domains of assemblies were predicted by Augustus (Stanke and Waack 2003). The DNA sequences of single-copy orthologs were used for phylogenomic reconstruction. These sequences were aligned in MUSCLE (Edgar 2004). We used Gblocks 0.91 b (Talavera and Castresana 2007) to remove the highly variable regions of the alignment of each ortholog. The minimum length of the conserved region was set to 10 ($-b4 = 10$) with all gaps were removed in these analyses.

We used two methods to reconstruct the phylogeny of *Niviventer* basing on SCOs. In the first method, we concatenated all SCOs together, and extracted SNP sites using SNP-sites (PaGe et al. 2016). Bayesian Markov chain Monte Carlo (MCMC) inferences using these SNP sites was conducted in MrBayes 3.2.2. Trees were visualized in FigTree 1.40 (Rambaut 2010). Secondly, we inferred species tree using the gene trees of 4,964 SCOs (at least presented in four species) in RaxML 8.2.12 (Stamatakis 2014) with 100 bootstraps and a GTRGAMMA model for each gene. The best tree for each gene was used to summarize species tree in ASTRAL5.7.3 (Zhang et al. 2018). This is one of the leading methods for inferring species trees from gene trees while accounting for gene tree discordance, which can be caused by incomplete lineage sorting, gene-flow between species etc.

Testing Phylogenetic Networks and Hybridization among Species

To reconstruct the phylogenetic network among *Niviventer*, we used the following four methods: 1) Autumn algorithm (Huson and Linz 2018) implemented in Dendroscope 3.7.2 (Huson and Scornavacca 2012), which computing minimum hybridization networks for a given pair of “realistic” rooted phylogenetic trees on overlapping taxa sets. Gene trees resulted from the SCOs were used in this analysis. 2 and 3) We inferred phylonetworks using maximum pseudolikelihood and Bayesian inference in Phylonet (Yu and Nakhleh 2015; Wen et al. 2016). 4) We reconstructed phylonetwork among species using Phylonetworks (Solís-Lemus et al. 2017, 2018). Gene trees of SCOs were used in these three methods.

Inferring Divergence Time and Geographical Evolutionary History

We established two data sets to inferring the divergence time of *Niviventer*. The first data set including SNP extracted the concatenated data of all SCOs using SNP-sites. Then we used the MTG data set, which included two more species *Niviventer* (*N. cremoriventer* and *N. rapit*) than the single-

copy ortholog data set, to infer the divergence time and geographical evolutionary history. Molecular dating was conducted in BEAST 1.8.4 (Drummond and Rambaut 2007). The divergence time of Murinae (16 Ma), and the age of Rattini (11.2 Ma) were used as calibration points in the present analyses (Aghová et al. 2018). The stability of the results was tested in Tracer (Rambaut and Drummond 2007). The phylogeny reconstructed in the above analyses was used for geographical evolutionary history inference in RASP 4 (Yu et al. 2020). We inferred the elevations evolution of *Niviventer* using the average values of their current distribution based on available collection records. All outgroup taxa were excluded from these analyses to avoid bias due to the distribution of outgroups.

Reconstructing Demographic History

We used two data sets to analyze the demographic history of different species within *Niviventer*. The first data set included CYTB sequences from 17 species, and the second data set included 15 assembled contig files for each species.

For the CYTB data, we used DnaSP v5 (Librado and Rozas 2009) to quantify the number of haplotypes in each species. We ran tests for Tajima's *D* (Tajima 1989), Fu and Li's *D* (Fu 1997), Fu and Li's *F* (Fu 1997), and Fu' *F* (Fu 1997) to assess whether the evolution of different species fit a neutral equilibrium. Significant and large negative values of Tajima's *D* and *F* values are indicative of population expansion, whereas positive values for these tests indicate a decrease in population size. Second, we tested the pairwise mismatch distribution for the signatures of the demographic expansion. A unimodal mismatch distribution is apparent when the population experiences a sudden expansion. In contrast, multimodal and ragged mismatch distributions are indicative of a stable or contracting population. Third, we reconstructed the demographic history of these species by using the CYTB sequences of each species to construct extended Bayesian skyline plots (EBSPs) in BEAST (Bouckaert et al. 2014). A strict molecular-clock model was used with substitution models and clock models unlinked among partitions in all the analyses. A range of 0.02–0.06 nucleotide changes per site per million years was used as the lower and upper values for the clock rate, as this range is commonly used for the mtDNA of small mammals (Martin and Palumbi 1993; Suzuki et al. 2015). We used 0.5 as a scaling factor in the population model because only the female mtDNA contributes to the effective population size. Divergence times inferred in the above analyses were used as the ranges of divergence times for each lineage. For all lineages, analyses were run for 80 million generations, sampling every 1,000 steps and discarding the first 25% of generations as burn-in. We performed each analysis twice to test the convergence of the results. For all analyses, the effective sample size (ESS) of all parameters exceeded 200.

Moreover, we used the pairwise sequential Markovian coalescent (PSMC) model (Li and Durbin 2011) to test demographic history based on individual contig files of the genomic data for each species. Since no reference genome for species of *Niviventer* were available in GenBank, we used the contig

files that were obtained in the above assemblies from MEGAHIT to regenerate 20 pseudochromosomes for each species. In this step, the contig files of each species were merged randomly to regenerate 20 pseudochromosomes in the FASTA file by using Fatoools in iTools (He et al. 2013). Then we mapped the clean reads back to the newly generated pseudochromosome data individually. Next, we used BWA (Li and Durbin 2009) and SAMtools (Li et al. 2009) (with the parameters samtools view -bS) to convert the aligned results to bam files. We sorted the bam files and built an index for the sorted file. We estimated genotype likelihoods with an adjusted mapping quality >50 (samtools mpileup -C50). We used BCFTools to identify the single-nucleotide polymorphisms (SNPs) (bcftools view -c). We used the file generated to conduct PSMC analysis (Li and Durbin 2011). We used “vcfutils.pl” to obtain a consensus genome sequence (vcfutils.pl vcf2fq -d 3 -D 100), in which -d is a command to exclude sites with a root-mean-square mapping quality <5 , and mapping depths >100 or <3 . We converted the format of consensus sequences by using fq2psmcfa (fq2psmcfa -q20). After the transformation, the population histories of each species were inferred by PSMC analysis (psmc -N25 -t15 -r5 -p "4 + 25 × 2 + 4 + 6). Since *Niviventer* is closely related to *Rattus*, we followed the studies of *Rattus* to use 0.5 year as the generation time, and 2.5×10^{-8} as the mean mutation rate for nuclear protein-coding genes according to previous studies (Teng et al. 2017; Zeng et al. 2018).

Identifying Genes under Positive Selection

DNA sequence files of each species annotated by Augustus in the above analyses were concatenated into one FASTA file for each species. We used TransDecoder v 5.5.0 (<http://transdecoder.github.io>) to identify Coding domain (CDs). We used PosiGene (Sahm et al. 2017) to scan positively selected genes (PSG) in each species. In the first running, *R. norvegicus* were used as anchor species and reference species. About 60,084 cds sequences of *R. norvegicus* were used as baits to assign homologous sequence of these genes in newly sequenced species into respective folders. In the formal analyses, the most closely related species of the target species was used as an anchor species. *Rattus norvegicus* and *M. musculus* was used as outgroup taxa. CD data sets for both species were downloaded from GenBank. There were three major steps during this analysis: 1) building the ortholog catalog based on CD sequences of *R. norvegicus* by using a best bidirectional BLAST hit criterion; 2) aligning these orthologs separately using PRANK (Loytynoja and Goldman 2005), removing highly divergent sequences, and producing a guide tree for the third step; and 3) identifying genes under positive selection using CODEML in PAML (Yang 2007). A multiple comparisons test was performed. Genes with adjusted P value <0.05 was used in the following analyses.

Adjusted $P < 0.05$ resulted in above analyses may induced from poor quality or misalignment of sequences. We realign each gene of all available species individually that was selected by PosiGene using MUSCLE, and manually check them by eye to make sure poorly sequenced data were excluded in the

final analyses, and the remaining sequences correctly aligned to the known sequence of *R. norvegicus* or *M. musculus*, and then can be translate into protein sequences correctly. Stop codons at the end of cds were excluded. We used CODEML in PAML to test the significance of positive selection on these genes individually. Branch-site mode in CODEML was used to test the significance of positive selection. MA model (model = 2, NSsite = 2, fix omega = 0) and MA null model (model = 2, NSsite = 2, fix omega = 1) were run on each alignment of selected genes from the above analyses to produce likelihood ratio test (LRT) scores, and then to determine P values using χ^2 tests.

Genes were considered PSGs if the tests resulted in a false discovery rate (FDR) of <0.05 with an adjusted P value of <0.05 . False discovery rate (FDR) correction was conducted in the R using the Benjaminiand Hochberg method. Moreover, we evaluated the correctness of sequences generated by Illumina using Sanger sequencing. Partial sequences of *SETD2* and *CYP8B1* were amplified and sequenced using primers listed in [supplementary table 8, Supplementary Material](#) online. MrBayes inferences of each gene that presented in more than five species were conducted to build tree for these positively selected genes.

GO Enrichment Analyses and Detection of Functional Interactions among Proteins

We performed Gene Ontology (GO) enrichment analysis by using the positively selected genes detected as described above, with ortholog catalog of Rat (*R. norvegicus*) as the background species. The analyses were performed with the online server ShinyGo v0.61 (Ge, Jung, et al. 2020). FDR correction was performed in the GO enrichment analysis. Shiny GO is an online tool for the discovery and visualization of enriched GO terms in user-provided gene lists.

Testing for Ecological Differentiation

To examine the effects of climate change on species range and speciation processes, we first built past (Last Interglacial, LIG, and Last Glacial Maximum, LGM), present, and future (2050, RCP8.5 scenario) ecological niche models (ENMs) using the MaxEnt 3.4.1 algorithm implemented in the ENMeval R package (Muscarella et al. 2014). We used 19 temperature- and precipitation-related variables downloaded from the worldclim database at a 2.5-min resolution for all periods. Because the correlations between climatic parameters in past, present, and future scenarios varied, we kept all 19 variables to ensure that our models were comparable. Nevertheless, MaxEnt is robust to predict collinearity, and therefore, such collinearity should not affect our results (Feng et al. 2019). Species occurrence was confined to confirmed museum specimens or genetically sampled individuals. For *N. rapit* and *N. tenaster*, we complemented our data set with museum records available through the Global Biodiversity Information Facility (GBIF) database (<https://www.gbif.org/>). After excluding duplicated localities, the available sample sizes for the species were *N. andersoni* ($n = 35$), *N. bukit* ($n = 7$), *N. confucianus* ($n = 65$), *N. cremoriventer* ($n = 20$), *N. eha* ($n = 28$), *N. excelsior* ($n = 12$), *N. fulvescens*

($n = 15$), *N. huang* ($n = 26$), *N. lotipes* ($n = 29$), *N. mekongis* ($n = 15$), *N. niviventer* ($n = 15$), *N. pianmaensis* ($n = 7$), *N. rapit* ($n = 17$), and *N. tenaster* ($n = 6$) (supplementary fig. 1, Supplementary Material online). We did not include *N. coninga*, *N. culturatus*, *N. fengi*, *N. gladiusmaculus*, and *N. brahma* in the climatic niche analyses because of their limited distribution records.

To test the performance of our models, we partitioned the localities into testing and training bins using the “checkerboard2” method for species with sample sizes >25 and the “jackknife” method for species with smaller sample sizes (Muscarella et al. 2014). About 10,000 background points were randomly selected for model training from a defined buffer area (Lat: $-10S$, $60N$; Long: $65E$, $140E$) that includes the entire distribution of the genus. For each species, we compared models with distinct complexities using regularization multipliers ranging from 0 to 5 with five combinations of feature classes (L, LQ, LQP, H, and LGH; where L = linear, Q = quadratic, H = hinge, and P = product), and ranked them via the second order corrected Akaike information criterion (AIC). The performance of the best model (smallest AIC) was evaluated using the area under the curve (AUC) (Mason and Graham 2002). All models showed AUC values closer to one (ranging from 0.8351 to 0.9877) (supplementary table 9, Supplementary Material online), indicating higher performance in discriminating species occurrence data from random background points (Phillips et al. 2004).

To compare past, current, and future niche models, we first converted the raw MaxEnt output into a logistic output, which resulted in a probability of presence varying from 0 to 1. This approach allows a direct comparison across distinct models (Phillips et al. 2006). Comparisons between past, present, and future modeled species range were based on binary maps defined by the 10th percentile training presence Cloglog threshold; grid cells with a logistic probability of presence value higher than this threshold were reclassified as “1,” indicating presence and those with a probability below the threshold were reclassified as “0” indicating absence.

To assess species range shifts over time we calculated the suitable area (in km^2) and assessed the direction of shifts for each modeled scenario based on the threshold maps. To evaluate the effect of climate on speciation, we combined our modeled species distribution ranges obtained using the Cloglog threshold presence maps with the genomic tree. We assessed the evolution of climatic tolerances in *Niviventer* by using the phyloclim R package (Heibl 2009) and investigated the relationship between time since divergence and species range overlap via age-range correlation (ARC) analysis using the ENMTools R package (Warren et al. 2010). ARC analysis sheds light on the role of allopatric or sympatric speciation on shaping genus current diversity (Fitzpatrick and Turelli 2006).

Supplementary Material

Supplementary data are available at *Molecular Biology and Evolution* online.

Acknowledgments

We appreciate valuable suggestions from Drs Arne Sahn, Shixia Xu, Fangluan Gao, Qiang Gao, Hua Chen, Chaochao Yan, Yu Wang, Yalin Cheng, and Chengmin Shi for data analyses. We also appreciate great help from anonymous reviewers and the editorial team. This work was sponsored by the Second Tibetan Plateau Scientific Expedition and Research Program (Nos. 2019QZKK0402, 2019QZKK0501) and the National Nature Science Fund of China (31872958). D.Y.G. and A.P.V. was supported by the Newton Advanced Fellowship of the Royal Society, United Kingdom (NA150142). A.V.A. is sponsored by the International Fellowship for Distinguished Scientists, Chinese Academy of Sciences (Ref. 2017VBA0027) and in part by grants-in-aid from the Ministry of Science and Higher Education of Russian (project AAAA-A19-119082990107-3). A.F. is financially supported by the Chinese Academy of Sciences President’s International Fellowship Initiative (2018PB0040/2021PB0021).

Author Contributions

D.Y.G., Q.S.Y., and A.P.V. designed research. D.Y.G., A.F., S.C.Y., S.K.P., and A.V.A. performed research and data analyses. D.Y.G., Z.X.W., L.L., A.V.A., J.L.C., L.X., X.L.J., and Q.S.Y. participated in sample collection. D.Y.G., A.F., A.V.A., L.L., A.P.V., and Q.S.Y. wrote the article.

Data Availability

Assembled sequences newly generated in the present study are available in GenBank (accession number MW191601–MW191697, MW193727–MW193744). Original sequence reads of genome data are available at the China National GeneBank (accession number CNP0001167).

References

- Aghová T, Kimura Y, Bryja J, Dobigny G, Granjon L, Kergoat GJ. 2018. Fossils know it best: using a new set of fossil calibrations to improve the temporal phylogenetic framework of murid rodents (Rodentia: Muridae). *Mol Biol Evol.* 128:98–111.
- Altschul SF, Gish W, Miller W, Myers EW, Lipman DJ. 1990. Basic local alignment search tool. *J Mol Biol.* 215(3):403–410.
- Aylon Y, Gershoni A, Rotkopf R, Biton IE, Porat Z, Koh AP, Sun X, Lee Y, Fiel M-I, Hoshida Y, et al. 2016. The *LATS2* tumor suppressor inhibits SREBP and suppresses hepatic cholesterol accumulation. *Genes Dev.* 30(7):786–797.
- Barnosky AD, Hadly EA, Bascompte J, Berlow EL, Brown JH, Fortelius M, Getz WM, Harte J, Hastings A, Marquet PA, Martinez ND, Mooers A, et al. 2012. Approaching a state shift in Earth’s biosphere. *Nature* 486(7401):52–58.
- Beyer TA, Werner S, Dickson C, Grose R. 2003. Fibroblast growth factor 22 and its potential role during skin development and repair. *Exp Cell Res.* 287(2):228–236.
- Bouckaert R, Heled J, Kuhnert D, Vaughan T, Wu CH, Xie D, Suchard MA, Rambaut A, Drummond AJ. 2014. BEAST 2: a software platform for Bayesian evolutionary analysis. *PLoS Comput Biol.* 10(4):e1003537.
- Buck L, Axel R. 1991. A novel multigene family may encode odorant receptors – a molecular-basis for odor recognition. *Cell* 65(1):175–187.
- Cao ZW, Zuo SQ, Gong ZD, Zhan L, Bian CL, Zhang PH, Yang H, Zhang JS, Zhao QM, Jia N, et al. 2010. Genetic analysis of a Hantavirus strain

- carried by *Niviventer confucianus* in Yunnan province. *China Virus Res.* 153(1):157–160.
- Carter H, Samayoa J, Hruban RH, Karchin R. 2010. Prioritization of driver mutations in pancreatic cancer using cancer-specific high-throughput annotation of somatic mutations (CHASM). *Cancer Biol Ther.* 10(6):582–587.
- Chen SF, Zhou YQ, Chen YR, Gu J. 2018. Fastp: an ultra-fast all-in-one FASTQ preprocessor. *Bioinformatics* 34(17):i884–i890.
- Chevin L-M, Lande R, Mace GM. 2010. Adaptation, plasticity, and extinction in a changing environment: towards a predictive theory. *PLoS Biol.* 8(4):e1000357.
- Dai XX, Jian C, Li N, Li DX. 2019. Characterization of the L genome segment of an orthohantavirus isolated from *Niviventer confucianus*. *Arch Virol.* 164(2):613–616.
- Dallmeyer A, Claussen M, Ni J, Cao X, Wang Y, Fischer N, Pfeiffer M, Jin L, Khon V, Wagner S, et al. 2017. Biome changes in Asia since the mid-Holocene – an analysis of different transient Earth system model simulations. *Clim Past.* 13 (2):107–134.
- Davis M, Faurby S, Svenning JC. 2018. Mammal diversity will take millions of years to recover from the current biodiversity crisis. *Proc Natl Acad Sci U S A.* 115(44):11262–11267.
- Deinum EE, Halligan DL, Ness RW, Zhang YH, Cong L, Zhang JX, Keightley PD. 2015. Recent evolution in *Rattus norvegicus* is shaped by declining effective population size. *Mol Biol Evol.* 32(10):2547–2558.
- Deng T, Wang XM, Fortelius M, Li Q, Wang Y, Tseng ZJ, Takeuchi GT, Saylor JE, Salla LK, Xie GP. 2011. Out of Tibet: pliocene woolly rhino suggests high-plateau origin of Ice Age megaherbivores. *Science* 333(6047):1285–1288.
- Denys C, Taylor PJ, Burgin CJ, Aplin KP, Fabre PH, Haslauer R, Woinarski JC, Breed WC, Menzies JR. 2016. Family Muridae. In: Wilson DE, Lacher TE, Mittermeier RA, editors. Handbook of the mammals of the world. 7. Barcelona: Lynx Edicions. p. 635–884.
- Dierckxsens N, Mardulyn P, Smits G. 2017. NOVOPlasty: de novo assembly of organelle genomes from whole genome data. *Nucleic Acids Res.* 45(4):e18.
- Drummond AJ, Rambaut A. 2007. BEAST: Bayesian evolutionary analysis by sampling trees. *BMC Evol Biol.* 7(1):214.
- Edgar RC. 2004. MUSCLE: multiple sequence alignment with high accuracy and high throughput. *Nucleic Acids Res.* 32(5):1792–1797.
- Feng X, Park DS, Liang Y, Pandey R, Papeş M. 2019. Collinearity in ecological niche modeling: confusions and challenges. *Ecol Evol.* 9(18):10365–10376.
- Filippou PS, Ren AH, Soosaipillai A, Safar R, Prassas I, Diamandis EP, Conner JR. 2020. Kallikrein-related peptidases protein expression in lymphoid tissues suggests potential implications in immune response. *Clin Biochem.* 77:41–47.
- Fitzpatrick BM, Turelli M. 2006. The geography of mammalian speciation: mixed signals from phylogenies and range maps. *Evolution* 60(3):601–615.
- Franks SJ, Hoffmann AA. 2012. Genetics of climate change adaptation. *Annu Rev Genet.* 46(1):185–208.
- Fu YX. 1997. Statistical tests of neutrality of mutations against population growth, hitchhiking and background selection. *Genetics* 147(2):915–925.
- Galetti M, Moleón M, Jordano P, Pires MM, Guimarães PR Jr, Pape T, Nichols E, Hansen D, Olesen JM, Munk M, et al. 2018. Ecological and evolutionary legacy of megafauna extinctions. *Biol Rev.* 93(2):845–862.
- Ge DY, Feijó A, Abramov A, Wen ZX, Liu ZJ, Cheng JL, Xia L, Lu L, Yang QS. 2020. Molecular phylogeny and morphological diversity of the *Niviventer fulvescens* species complex with emphasis on species from China. *Zool J Linn Soc.* 191(2):528–547.
- Ge DY, Lu L, Xia L, Du YB, Wen ZX, Cheng JL, Abramov AV, Yang QS. 2018. Molecular phylogeny, morphological diversity, and systematic revision of a species complex of common wild rat species in China (Rodentia, Murinae). *J Mammal.* 99(6):1350–1374.
- Ge DY, Wen ZX, Xia L, Zhang ZQ, Erbajeva M, Huang CM, Yang QS. 2013. Evolutionary history of lagomorphs in response to global environmental change. *PLoS One* 8(4):e59668.
- Ge SX, Jung D, Yao R. 2020. ShinyGO: a graphical gene-set enrichment tool for animals and plants. *Bioinformatics* 36(8):2628–2629.
- Ge XY, Yang WH, Pan H, Zhou JH, Han X, Zhu GJ, Desmond JS, Daszak P, Shi ZL, Zhang YZ. 2016. Fugong virus, a novel hantavirus harbored by the small oriental vole (*Eothenomys leucus*) in China. *Virol J.* 13(1):27.
- Geng A, Qiu R, Murai K, Liu J, Wu X, Zhang H, Farhoodi H, Duong N, Jiang M, Yee JK, et al. 2018. *KIF20A/MKLP2* regulates the division modes of neural progenitor cells during cortical development. *Nat Commun.* 9(1):2707.
- Guzzetta G, Tagliapietra V, Perkins SE, Haufler HC, Poletti P, Merler S, Rizzoli A. 2017. Population dynamics of wild rodents induce stochastic fadeouts of a zoonotic pathogen. *J Anim Ecol.* 86(3):451–459.
- He W, Zhao SC, Liu X, Dong SS, Lv JX, Liu DH, Wang J, Meng Z. 2013. ReSeqTools: an integrated toolkit for large-scale next-generation sequencing based resequencing analysis. *Genet Mol Res.* 12(4):6275–6283.
- Heibl C. 2009. phyloclim: integrating phylogenetics and climatic niche modelling. R package version 0.0.1.
- Hoffmann AA, Sgro CM. 2011. Climate change and evolutionary adaptation. *Nature* 470(7335):479–485.
- Hu XQ, Li SG, Liu H, Wang J, Hua RM. 2014. Diversity and distribution of host animal species of hantavirus and risk to human health in Jiuha mountain area, China. *Biomed Environ Sci.* 27(11):849–857.
- Huson DH, Linz S. 2018. Autumn algorithm-computation of hybridization networks for realistic phylogenetic trees. *IEEE/ACM Trans Comput Biol Bioinf.* 15 (2):398–410.
- Huson DH, Scornavacca C. 2012. Dendroscope 3: an interactive tool for rooted phylogenetic trees and networks. *Syst Biol.* 61(6):1061–1067.
- Irwin D, Kocher T, Wilson A. 1991. Evolution of the cytochrome b gene of mammals. *J Mol Evol.* 32(2):128–144.
- Jahan A, Chiang JY. 2005. Cytokine regulation of human sterol 12alpha-hydroxylase (CYP8B1) gene. *Am J Physiol Gastrointest Liver Physiol.* 288(4):G685–G695.
- Jing MD, Yu HT, Bi X, Lai YC, Jiang W, Huang L. 2014. Phylogeography of Chinese house mice (*Mus musculus musculus/castaneus*): distribution, routes of colonization and geographic regions of hybridization. *Mol Ecol.* 23(17):4387–4405.
- Johansson CC, Dahle MK, Blomqvist SR, Gronning LM, Aandahl EM, Enerback S, Tasken K. 2003. A winged helix forkhead (FOXO2) tunes sensitivity to cAMP in T lymphocytes through regulation of cAMP-dependent protein kinase R1alpha. *J Biol Chem.* 278(19):17573–17579.
- Kriventseva EV, Kuznetsov D, Tegenfeldt F, Manni M, Dias R, Simao FA, Zdobnov EM. 2019. OrthoDB v10: sampling the diversity of animal, plant, fungal, protist, bacterial and viral genomes for evolutionary and functional annotations of orthologs. *Nucleic Acids Res.* 47(D1):D807–D811.
- Lai CH, Smith AT. 2003. Keystone status of plateau pikas (*Ochotona curzoniae*): effect of control on biodiversity of native birds. *Biod Conserv.* 12(9):1901–1912.
- Lanfear R, Frandsen PB, Wright AM, Senfeld T, Calcott B. 2017. PartitionFinder 2: new methods for selecting partitioned models of evolution for molecular and morphological phylogenetic analyses. *Mol Biol Evol.* 34(3):772–773.
- Latif A, Liu BY, Chen Z, Sun Y, Shi YL, Zong J, Li JJ, Ren CP, Zhang XC, Liu XN, et al. 2017. *Orientia tsutsugamushi* infection in rodents in Anhui Province of China. *Infect Genet Evol.* 56:14–18.
- Leis SA, Leslie DM Jr, Engle DM, Fehmi JS. 2008. Small mammals as indicators of short-term and long-term disturbance in mixed prairie. *Environ Monit Assess.* 137(1–3):75–84.
- Leng ZG, Lin SJ, Wu ZR, Guo YH, Cai L, Shang HB, Tang H, Xue YJ, Lou MQ, Zhao W, et al. 2017. Activation of DRD5 (Dopamine receptor D5) inhibits tumor growth by autophagic cell death. *Autophagy* 13(8):1404–1419.
- Li D, Liu CM, Luo R, Sadakane K, Lam TW. 2015. MEGAHIT: an ultra-fast single-node solution for large and complex metagenomics assembly via succinct de Bruijn graph. *Bioinformatics* 31(10):1674–1676.
- Li H, Durbin R. 2009. Fast and accurate short read alignment with Burrows-Wheeler transform. *Bioinformatics* 25(14):1754–1760.

- Li H, Durbin R. 2011. Inference of human population history from individual whole-genome sequences. *Nature* 475(7357):493–496.
- Li H, Handsaker B, Wysoker A, Fennell T, Ruan J, Homer N, Marth G, Abecasis G, Durbin R, 1000 Genome Project Data Processing Subgroup. 2009. The sequence alignment/map format and SAMtools. *Bioinformatics* 25(16):2078–2079.
- Li J, Duns G, Westers H, Sijmons R, van den Berg A, Kok K. 2016. *SETD2*: an epigenetic modifier with tumor suppressor functionality. *Oncotarget* 7(31):50719–50734.
- Li J, Labbadia J, Morimoto RI. 2017. Rethinking *HSF1* in stress, development, and organismal Health. *Trends Cell Biol.* 27(12):895–905.
- Li Q, Xie GP, Takeuchi GT, Deng T, Tseng ZJ, Grohe C, Wang XM. 2014. Vertebrate fossils on the roof of the world: biostratigraphy and geochronology of high-elevation Kunlun Pass Basin, northern Tibetan Plateau, and basin history as related to the Kunlun strike-slip fault. *Palaeogeogr Palaeocl.* 411:46–55.
- Li Q, Zhou XY, Ni XJ, Fu BH, Deng T. 2020. Latest middle Miocene fauna and flora from Kumkol Basin of northern Qinghai-Xizang Plateau and paleoenvironment. *Sci China Earth Sci.* 63(2):188–201.
- Li SN, He JC, Liu YP, Yang J. 2020. *FGF22* promotes generation of ribbon synapses through downregulating *MEF2D*. *Aging* 12(7):6456–6466.
- Li Z, Chen YN, Li WH, Deng HJ, Fang GH. 2015. Potential impacts of climate change on vegetation dynamics in Central Asia. *J Geophys Res Atmos.* 120(24):12345–12356.
- Librado P, Rozas J. 2009. DnaSP v5: a software for comprehensive analysis of DNA polymorphism data. *Bioinformatics* 25(11):1451–1452.
- Lin XD, Wang W, Guo WP, Zhang XH, Xing JG, Chen SZ, Li MH, Chen Y, Xu JG, Plyusnin A, et al. 2012. Cross-species transmission in the speciation of the currently known Murinae-associated hantaviruses. *J Virol.* 86(20):11171–11182.
- Liu DY, Liu J, Liu BY, Liu YY, Xiong HR, Hou W, Yang ZQ. 2017. Phylogenetic analysis based on mitochondrial DNA sequences of wild rats, and the relationship with Seoul virus infection in Hubei, China. *Virol Sin.* 32(3):235–244.
- Lossow K, Hubner S, Roudnitzky N, Slack JP, Pollastro F, Behrens M, Meyerhof W. 2016. Comprehensive analysis of mouse bitter taste receptors reveals different molecular receptive ranges for orthologous receptors in mice and humans. *J Biol Chem.* 291(29):15358–15377.
- Loytynoja A, Goldman N. 2005. An algorithm for progressive multiple alignment of sequences with insertions. *Proc Natl Acad Sci U S A.* 102(30):10557–10562.
- Lu L, Ge DY, Chesters D, Ho SYW, Ma Y, Li GC, Wen ZX, Wu YJ, Wang J, Xia L, et al. 2015. Molecular phylogeny and the underestimated species diversity of the endemic white-bellied rat (Rodentia: Muridae: *niviventer*) in Southeast Asia and China. *Zool Scr.* 44(5):475–494.
- Malhi Y, Doughty CE, Galetti M, Smith FA, Svenning JC, Terborgh JW. 2016. Megafauna and ecosystem function from the Pleistocene to the Anthropocene. *Proc Natl Acad Sci U S A.* 113(4):838–846.
- Martin AP, Palumbi SR. 1993. Body size, metabolic rate, generation time, and the molecular clock. *Proc Natl Acad Sci U S A.* 90(9):4087–4091.
- Mason SJ, Graham NE. 2002. Areas beneath the relative operating characteristics (ROC) and relative operating levels (ROL) curves: statistical significance and interpretation. *Q J R Meteorol Soc.* 128(584):2145–2166.
- Masuzawa T, Takada N, Kudeken M, Fukui T, Yano Y, Ishiguro F, Kawamura Y, Imai Y, Ezaki T. 2001. *Borrelia sinica* sp. nov., a Lyme disease-related *Borrelia* species isolated in China. *Int J Syst Evol Microbiol.* 51(5):1817–1824.
- McClelland GTW, Altwegg R, Aarde RJ, Ferreira S, Burger AE, Chown SL. 2018. Climate change leads to increasing population density and impacts of a key island invader. *Ecol Appl.* 28(1):212–224.
- McClenachan L, Cooper AB, Dulvy NK. 2016. Rethinking trade-driven extinction risk in marine and terrestrial megafauna. *Curr Biol.* 26(12):1640–1646.
- Meng GL, Li YY, Yang CT, Liu SL. 2019. MitoZ: a toolkit for animal mitochondrial genome assembly, annotation and visualization. *Nucleic Acids Res.* 47(11):e63.
- Muscarella R, Galante PJ, Soley-Guardia M, Boria RA, Kass JM, Uriarte M, Anderson RP. 2014. ENMeval: an R package for conducting spatially independent evaluations and estimating optimal model complexity for Maxent ecological niche models. *Methods Ecol Evol.* 5(11):1198–1205.
- Musser GG. 1981. Results of the Archbold Expeditions. No. 105. Notes on systematics of Indo-Malayan murid rodents, and descriptions of a new genera and species from Ceylon, Sulawesi, and the Philippines. *B Am Mus Nat Hist.* 168:229–334.
- Musser GG, Carleton MD. 2005. Superfamily Muroidea. In: Wilson DE, Reeder DM, editors. *Mammal species of the world a taxonomic and geographic reference*. Baltimore: Johns Hopkins University Press. p. 894–1531.
- Page AJ, Taylor B, Delaney AJ, Soares J, Seemann T, Keane JA, Harris SR. 2016. SNP-sites: rapid efficient extraction of SNPs from multi-FASTA alignments. *Microbial Genomics.* 2(4):e000056.
- Patel RK, Jain M. 2012. NGS QC toolkit: a toolkit for quality control of next generation sequencing data. *PLoS One* 7(2):e30619.
- Phillips SJ, Anderson RP, Schapire RE. 2006. Maximum entropy modeling of species geographic distributions. *Ecol Model.* 190(3–4):231–259.
- Phillips SJ, Dudík M, Schapire RE. 2004. A maximum entropy approach to species distribution modeling. Proceedings of the Twenty-First International Conference on Machine Learning Banff, Alberta (Canada): Association for Computing Machinery. p. 83.
- Puckett EE, Park J, Combs M, Blum MJ, Bryant JE, Caccone A, Costa F, Deinum EE, Esther A, Himsworth CG, Keightley PD, et al. 2016. Global population divergence and admixture of the brown rat (*Rattus norvegicus*). *Proc Biol Sci.* 283: 20161762.
- Rabiee MH, Mahmoudi A, Siahsarvie R, Krystufek B, Mostafavi E. 2018. Rodent-borne diseases and their public health importance in Iran. *PLoS Negl Trop Dis.* 12(4):e0006256.
- Raharinsoy V, Olive MM, Andriamiramanana FM, Andriamandimby SF, Ravalohery JP, Andriamamonjy S, Filippone C, Rakoto DAD, Telfer S, Heraud JM. 2018. Geographical distribution and relative risk of *Anjzorobe* virus (Thailand orthohantavirus) infection in black rats (*Rattus rattus*) in Madagascar. *Virol J.* 15(1):83.
- Rambaut A. 2010. FigTree v1.40. Edinburgh: Institute of Evolutionary Biology, University of Edinburgh. Available from: <http://tree.bio.ed.ac.uk/software/figtree/>.
- Rambaut A, Drummond AJ. 2007. Tracer v1.5. Available from: <http://beast.bio.ed.ac.uk/Tracer>.
- Ronquist F, Teslenko M, van der Mark P, Ayres DL, Darling A, Höhna S, Larget B, Liu L, Suchard MA, Huelsenbeck JP. 2012. MrBayes 3.2: efficient Bayesian phylogenetic inference and model choice across a large model space. *Syst Biol.* 61(3):539–542.
- Rowe RJ, Terry RC. 2014. Small mammal responses to environmental change: integrating past and present dynamics. *J Mammal.* 95(6):1157–1174.
- Ruthala K, Gadi J, Lee JY, Yoon H, Chung HJ, Kim MH. 2011. Hoxc8 downregulates Mgl1 tumor suppressor gene expression and reduces its concomitant function on cell adhesion. *Mol Cells.* 32(3):273–279.
- Sahm A, Bens M, Platzer M, Szafranski K. 2017. PosiGene: automated and easy-to-use pipeline for genome-wide detection of positively selected genes. *Nucleic Acids Res.* 45(11):e100.
- Saito-Ito A, Takada N, Ishiguro F, Fujita H, Yano Y, Ma XH, Chen ER. 2008. Detection of Kobe-type *Babesia* microti associated with Japanese human babesiosis in field rodents in central Taiwan and southeastern mainland China. *Parasitology* 135(6):691–699.
- Schmieder R, Edwards R. 2011. Quality control and preprocessing of metagenomic datasets. *Bioinformatics* 27(6):863–864.
- Shi G, Jiang N, Yao LQ. 2018. Land use and cover change during the rapid economic growth period from 1990 to 2010: a case study of Shanghai. *Sustainability* 10(2):426.
- Simão FA, Waterhouse RM, Ioannidis P, Kriventseva EV, Zdobnov EM. 2015. BUSCO: assessing genome assembly and annotation completeness with single-copy orthologs. *Bioinformatics* 31(19):3210–3212.
- Smith AT, Foggini JM. 1999. The plateau pika (*Ochotona curzoniae*) is a keystone species for biodiversity on the Tibetan plateau. *Anim Cons.* 2(4):235–240.

- Solís-Lemus C, Bastide P, Ané C. 2017. PhyloNetworks: a package for phylogenetic networks. *Mol Biol Evol.* 34(12):3292–3298.
- Stamatakis A. 2014. RAxML Version 8: a tool for phylogenetic analysis and post-analysis of large phylogenies. *Bioinformatics* 30(9):1312–1313.
- Stanke M, Waack S. 2003. Gene prediction with a hidden Markov model and a new intron submodel. *Bioinformatics* 19(Suppl 2):ii215–i225.
- Stuart AJ, Kosintsev PA, Higham TF, Lister AM. 2004. Pleistocene to Holocene extinction dynamics in giant deer and woolly mammoth. *Nature* 431(7009):684–689.
- Suzuki TA, Phifer-Rixey M, Mack KL, Sheehan MJ, Lin D, Bi K, Nachman MW. 2019. Host genetic determinants of the gut microbiota of wild mice. *Mol Ecol.* 28(9):2378–3207.
- Suzuki Y, Tomozawa M, Koizumi Y, Tsuchiya K, Suzuki H. 2015. Estimating the molecular evolutionary rates of mitochondrial genes referring to Quaternary ice age events with inferred population expansions and dispersals in Japanese *Apodemus*. *BMC Evol Biol.* 15(1):187.
- Tajima F. 1989. Statistical method for testing the neutral mutation hypothesis by DNA polymorphism. *Genetics* 123(3):585–595.
- Talavera G, Castresana J. 2007. Improvement of phylogenies after removing divergent and ambiguously aligned blocks from protein sequence alignments. *Syst Biol.* 56(4):564–577.
- Teng HJ, Zhang YH, Shi CM, Mao FB, Cai WS, Lu L, Zhao FQ, Sun ZS, Zhang JX. 2017. Population genomics reveals speciation and introgression between brown Norway rats and their sibling species. *Mol Biol Evol.* 34(9):2214–2228.
- Tseng ZJ, Li Q, Wang XM. 2013. A new cursorial *Hyena* from Tibet, and analysis of biostratigraphy, paleozoogeography, and dental morphology of *Chasmaporthetes* (Mammalia, Carnivora). *J Vert Paleon.* 33(6):1457–1471.
- Voskarides K. 2018. Combination of 247 genome-wide association studies reveals high cancer risk as a result of evolutionary adaptation. *Mol Biol Evol.* 35(2):473–485.
- Wang H, Yoshimatsu K, Ebihara H, Ogino M, Araki K, Kariwa H, Wang Z, Luo Z, Li D, Hang C, et al. 2000. Genetic diversity of hantaviruses isolated in China and characterization of novel hantaviruses isolated from *Niviventer confucianus* and *Rattus rattus*. *Virology* 278(2):332–345.
- Wang XM, Li Q, Takeuchi GT. 2016. Out of Tibet: an early sheep from the Pliocene of Tibet, *Protovis himalayensis*, genus and species nov (Bovidae, Caprini), and origin of Ice Age mountain sheep. *J Vert Paleon.* 36:e1169190.
- Wang XM, Li Q, Xie GP, Saylor JE, Tseng ZJ, Takeuchi GT, Deng T, Wang Y, Hou S, Liu J, et al. 2013. Mio-Pleistocene Zanda Basin biostratigraphy and geochronology, pre-Ice Age fauna, and mammalian evolution in western Himalaya. *Palaeogeogr Palaeoclimatol.* 374:81–95.
- Wang XM, Li Q, Xie GP. 2015. Earliest record of Sinicuon in Zanda Basin, southern Tibet and implications for hypercarnivores in cold environments. *Quat Intern.* 355:3–10.
- Wang XM, Tseng ZJ, Li Q, Takeuchi GT, Xie GP. 2014. From ‘third pole’ to north pole: a Himalayan origin for the arctic fox. *Proc Biol Sci.* 281(1787):20140893.
- Wang XM, Wang Y, Li Q, Tseng ZJ, Takeuchi GT, Deng T, Xie GP, Chang MM, Wang N. 2015. Cenozoic vertebrate evolution and paleoenvironment in Tibetan Plateau: progress and prospects. *Gondwana Res.* 27(4):1335–1354.
- Wang XY, Liang D, Jin W, Tang MK, Shalayiwi Liu SY, Zhang P. 2020. Out of Tibet: genomic perspectives on the evolutionary history of extant pikas. *Mol Biol Evol.* 37(6):1577–1592.
- Warren DL, Glor RE, Turelli M. 2010. ENMTools: a toolbox for comparative studies of environmental niche models. *Ecography* 33:607–611.
- Wen DQ, Yu I, Nakhleh L. 2016. Bayesian Inference of reticulate phylogenies under the multispecies network coalescent. *PLoS Genet.* 12(5):e1006006.
- Xu Q, Xiang Y, Wang Q, Wang L, Brind’Amour J, Bogutz AB, Zhang Y, Zhang B, Yu G, Xia W, et al. 2019. SETD2 regulates the maternal epigenome, genomic imprinting and embryonic development. *Nat Genet.* 51(5):844–856.
- Yang ZH. 2007. PAML 4: phylogenetic analysis by maximum likelihood. *Mol Biol Evol.* 24(8):1586–1591.
- Yin YP, Tang LN, Zhang JB, Tang B, Li ZY. 2011. Molecular cloning and gene expression analysis of Ercc6l in Sika deer (*Cervus nippon hortulorum*). *PLoS One* 6(6):e20929.
- Yu Y, Blair C, He XJ. 2020. RASP 4: ancestral state reconstruction tool for multiple genes and characters. *Mol Biol Evol.* 37(2):604–606.
- Yu Y, Nakhleh L. 2015. A maximum pseudo-likelihood approach for phylogenetic networks. *BMC Genomics* 16 (S10):S10.
- Zeng L, Ming C, Li Y, Su LY, Su YH, Otecko NO, Dalecky A, Donnellan S, Aplin K, Liu XH, et al. 2018. Out of Southern East Asia of the brown rat revealed by large-scale genome sequencing. *Mol Biol Evol.* 35(1):149–158.
- Zhang B, He K, Wan T, Chen P, Sun GZ, Liu SY, Nguyen TS, Lin LK, Jiang XL. 2016. Multi-locus phylogeny using topotype specimens sheds light on the systematics of *Niviventer* (Rodentia, Muridae) in China. *BMC Evol Biol.* 16(1):261.
- Zhang C, Maryam R, Erfan S, Siavash M. 2018. ASTRAL-III: polynomial time species tree reconstruction from partially resolved gene trees. *BMC Bioinformatics* 19 (S6):153.
- Zhang P, Ao H, Dekkers MJ, Li YX, An ZS. 2016. Late Oligocene–Early Miocene magnetochronology of the mammalian faunas in the Lanzhou Basin—environmental changes in the NE margin of the Tibetan Plateau. *Sci Rep.* 6(1):38023.